

**Early Damage Detection in Periodically Assembled Trusses Using Impulse
Response Method**

by

Onur Can
B.S. (Istanbul Technical University) 2015

Thesis submitted in partial fulfillment of the requirements
for the degree of Master of Science in Civil Engineering
in the Graduate College of the
University of Illinois at Chicago, 2017

Chicago, Illinois

Defense Committee:

Dr. Didem Ozevin, Chair and Advisor

Dr. Farhad Ansari, Civil and Materials Engineering

Dr. Mustafa Mahamid, Civil and Materials Engineering

Copyright by

Onur Can

2017

ACKNOWLEDGMENTS

This research is supported by National Science Foundation, Grant CMMI 1552375, entitled CAREER: Engineered Spatially Periodic Structure Design Integrated with Damage Detection Philosophy. I would like to thank the organization for their outstanding support. Also, I would like to thank Civil & Materials Department and Physics Department at University of Illinois at Chicago for making my Master's degree possible.

I would like to express my deepest appreciation to my advisor Dr. Didem Ozevin for her endless endorsement of my MS study and research. Her profound knowledge and supervision guided me in every moment of my study. In addition to my advisor, genuine thanks to my thesis committee members: Dr. Farhad Ansari and Dr. Mustafa Mahamid for their time, discussion and inquiry. In the end, I would like to thank to my labmates: Minoo Kabir, Zeynab Abbasi, Lu Zhang, Amir Mostavi, Ashley Newton and Hanie Kazari for their support.

TABLE OF CONTENTS

<u>CHAPTER</u>		<u>PAGE</u>
1	INTRODUCTION	1
1.1	Statement of Problem	1
1.2	Research Objective	2
1.3	Structure of Thesis	2
2	APPLICATION OF GENETIC ALGORITHM TO TRUSS OPTIMIZATION WITH PERIODICITY	4
2.1	Introduction	4
2.2	General Description of Genetic Algorithm	5
2.2.1	Formulation of Optimization Problem in Genetic Algorithm	6
2.2.1.1	Design Variables (Genes)	6
2.2.1.2	Objective Function (Fitness)	6
2.2.1.3	Constraints	7
2.2.2	Operators in Genetic Algorithm	8
2.2.3	Parameters in Genetic Algorithm	11
2.2.4	Optimization Examples Using Genetic Algorithm	11
2.2.4.1	Size Optimization of 10-Element Planar Truss	11
2.2.4.2	Size Optimization of 10-Bay Periodic Truss Bridge	14
2.2.5	Summary	18
3	IMPULSE RESPONSE METHOD TO PERIODICALLY ASSEMBLED TRUSSES	20
3.1	Introduction	20
3.2	Numerical Results	22
3.2.1	Influence of Number of Unit Cells in Periodicity	22
3.2.2	Experimental Truss Configuration	27
3.2.3	Impulse Response of 2D Truss Using COMSOL Multiphysics Software	28
3.2.3.1	Pristine Condition	28
3.2.3.2	Damaged Condition	29
3.3	Experimental Results	35
3.3.1	Experimental Setup	35
3.3.2	Pristine Condition	36
3.3.3	Damaged Condition	39
3.3.4	Calculation of Damping Using Q Factor Method	46
3.3.5	Comparison between Numerical and Experimental Results	47
3.4	Summary	48

TABLE OF CONTENTS (Continued)

<u>CHAPTER</u>		<u>PAGE</u>
4	CONCLUSIONS	50
	4.1 Summary	50
	4.2 Findings	51
	4.3 Future Work	51
	CITED LITERATURE	53
	VITA	56

LIST OF TABLES

<u>TABLE</u>		<u>PAGE</u>
I	Material properties of 10-element planar truss.	12
II	Comparison of the weight minimization results.	13
III	Total load for each bay of the truss.	14
IV	Materials properties (ASTM A992 Steel).	15
V	Weight minimization results of the truss.	17
VI	Weight minimization results of the truss.	18
VII	Material properties and cross sectional areas of the bar elements.	28
VIII	Peak energy ratio comparison between numerical and experimental model for 25% stiffness reduction.	48

LIST OF FIGURES

FIGURE		PAGE
1	Genetic algorithm flow chart.	8
2	10-element planar truss.	13
3	Load distribution along the truss, x-z view.	15
4	Different periodic assemblies of unit cells; (a) topology 1, (b) topology 2, (c) topology 3.	23
5	The impulse source using the impact hammer; (a) time domain, (b) frequency domain.	24
6	Impulse response of truss topology 1; (a) 5 cells, (b) 15 cells, (c) 30 cells, (d) 100 cells.	24
7	Impulse response of truss topology 2; (a) 5 cells, (b) 15 cells, (c) 30 cells, (d) 100 cells.	25
8	Impulse response of truss topology 3; (a) 5 cells, (b) 15 cells, (c) 30 cells, (d) 100 cells.	26
9	Truss configuration.	27
10	Numerical impulse responses of three adjacent unit cells for the pristine truss.	29
11	3D solid models of damaged elements; (a) pristine, (b) damaged. . .	30
12	Numerical impulse responses when damage is introduced to member in unit cell 1; (a) unit cell 1 response, (b) unit cell 2 response, (c) unit cell 3 response.	32
13	Numerical impulse responses when damage is introduced to member in unit cell 2; (a) unit cell 1 response, (b) unit cell 2 response, (c) unit cell 3 response.	33
14	Numerical impulse responses when damage is introduced to member in unit cell 3; (a) unit cell 1 response, (b) unit cell 2 response, (c) unit cell 3 response.	34
15	Experimental setup; (a) connection detail of the equipment, (b) bridge model.	36
16	Time histories of the repeated impulse response results for; (a) cell 1, (b) cell 2, (c) cell 3, (d) the comparison of averaged waveforms of each unit cell.	37
17	Frequency spectra of the repeated impulse response results; (a) cell 1, (b) cell 2, (c) cell 3, (d) the comparison of averaged frequency spectra of each unit cell.	38
18	Time histories of three unit cells when damage member is introduced in cell 1; (a) cell 1, (b) cell 2, (c) cell 3.	40
19	Time histories of three unit cells when damage member is introduced in cell 2; (a) cell 1, (b) cell 2, (c) cell 3.	41

LIST OF FIGURES (Continued)

<u>FIGURE</u>		<u>PAGE</u>
20	Time histories of three unit cells when damage member is introduced in cell 3; (a) cell 1, (b) cell 2, (c) cell 3.	42
21	FFT results of five different impulse response of three adjacent unit cells when damage member is introduced in cell 1; (a) cell 1, (b) cell 2, (c) cell 3.	43
22	FFT results of five different impulse response of three adjacent unit cells when damage member is introduced in cell 2; (a) cell 1, (b) cell 2, (c) cell 3.	44
23	FFT results of five different impulse response of three adjacent unit cells when damage member is introduced in cell 3; (a) cell 1, (b) cell 2, (c) cell 3.	45
24	Q factor method; (a) notation, (b) cell 2 response in dB scale.	46
25	Peak energies for 10-50% stiffness reductions in numerical model; (a) damage in unit cell 1, (b) damage in unit cell 2, (c) damage in unit cell 3.	47

SUMMARY

The objective of this research is to apply genetic algorithms (GA) for optimizing truss geometry with inducing periodicity and develop impulse-response based nondestructive evaluation approach using the advantage of periodic system design. Size optimization refers to a minimizing of cross sectional areas of the elements for a given topology of a structural system. The topology of a truss system is inspired from periodic lattices where elements periodically repeat themselves. In the optimization algorithm cross sectional areas of the truss elements are treated as a discrete design variable. According to the design variable, genetic algorithm attempts to find minimum weight of the structure by satisfying certain conditions such as tensile strength, compression strength and displacement of the structural elements. Using the optimized structural configuration with periodic arrangement of truss members, the impulse-response method is applied to identify the structural state of each repeating unit cell. The main hypothesis is that each unit cell has similar frequency response at the undamaged state. Once damage forms in a unit cell, its behavior deviates from the unit cell behavior. The approach has been numerically and experimentally demonstrated. The numerical models have been built using COMSOL Multiphysics software in the frequency domain. Numerical results include the impulse responses of the trusses with different numbers of unit cells and three different unit cell topologies for pristine and damaged conditions. In the experimental study, a steel truss bridge with eight repeating unit cells (one of the numerically modeled configurations) is built and tested using impact hammer and accelerometer. The positions of the impact hammer and accelerometer are

SUMMARY (Continued)

moved to each unit cell to record the frequency response and observe the periodic behavior. A damage is then introduced to a unit cell, and the deviance from the periodic behavior is observed in that unit cell as predicted. The developed approach allows nondestructive testing of periodically placed truss systems without baseline by simply comparing the frequency response of each unit cell.

CHAPTER 1

INTRODUCTION

1.1 Statement of Problem

The achievement of the best solution often comes together with the challenge of selecting between different design factors: therefore, optimization is inherently involved into the design process [1]. In general, optimization can be subcategorized into three main concepts: load-carrying capacity (safety), producibility and economy [2]. These three concepts are interrelated with each other and affect the cost of structure. In this research, load-carrying capacity is studied and the structural cost is naturally included into the optimization problem. There are certain criteria for the purpose of the structure functionality, which are specified in the design codes. In the conventional design process, these criteria are taken into account one by one. However, in order to achieve the best solution, in other words the most economical outcome, these criteria have to be considered simultaneously. Genetic algorithm (GA) allows to treat them at once as constraints in an efficient way. It is essential to say that all kinds of designs without optimization are deficient in terms of economy. Another issue that engineers face is lifespan of structures. All structures have a certain service lifespan due to deterioration of their materials. After that, structures have to be retrofitted or demolished. The determination of structural state and the prioritization for repair can be achieved by periodically recorded nondestructive evaluation (NDE) data. NDE provides real time inspection by using data ob-

tained from sensors. A damage in the structural members can be diagnosed and replaced with new elements, thus the lifespan of the structure can be increased. Generally speaking, design optimization and NDE are considered as two different disciplines. In fact, these two disciplines must be treated together considering the interaction of the structural design and nondestructive evaluation data. This new perspective not only gives the most feasible solution, but also considers future structural design concepts as “design for NDE”.

1.2 Research Objective

The main objective of this research is to integrate the design optimization and NDE approach into the same platform. It is necessary to study them concurrently. The optimization of steel structures relies on minimizing the total weight of the structure. This minimization problem can be readily done by the GA optimization. Since GA allows the use of constraints and does not require any derivation of function, it is a proper and efficient technique for structural optimization. The periodic assembly of the truss system is imposed as a constraint in the optimization process. By using periodicity, finite element model can be reduced greatly by repetitive finite element models. The influence of periodic assembly on the NDE method used in this study (impulse response method) is numerically and experimentally demonstrated.

1.3 Structure of Thesis

Chapter 2 begins with the background of optimization, literature review of genetic algorithm and its applications, and benchmark example for soundness of the method. Chapter 3 presents numerical and experimental studies of periodically assembled steel trusses using the

impulse response method. Finally, chapter 4 discusses the major conclusions of the research and recommendations for future work.

CHAPTER 2

APPLICATION OF GENETIC ALGORITHM TO TRUSS OPTIMIZATION WITH PERIODICITY

2.1 Introduction

A structure is defined as the constitution of materials in order to carry loads. Optimization refers to accomplishing the structural design in a best way. Therefore, structural optimization answers the question of how the loads can be transmitted to the ground in the best way. The best is not the same for all optimization problems. For this reason, it is necessary to define an appropriate best to achieve an optimal solution. The definition of the best is fulfilled by an objective function in GA. However, it is not sufficient to converge to a feasible solution, thus the optimization problem must be constrained. Design manuals and other structural requirements become a part of this method in terms of constraints. The objective in the truss optimization is minimizing the weight of the structure. Minimum weight criterion refers to the most economical solution since less materials will be used in the construction. Structural optimization is subcategorized into three: size, shape and topology. Firstly, size optimization indicates that the smallest cross sectional areas of the members which are permitted are used in the structure. Secondly, shape optimization searches for the optimum joint arrangement. Thirdly, topology optimization refers to best connectivity between existing joints while cross sectional areas of the members and joints' coordinates are fixed [3]. There are various optimization methods,

e.g. sequential linear programming (SLP) [4], Newton's method [5], gradient based method [6] and heuristic methods [7]. In this thesis, genetic algorithm is used as a heuristic optimization method. The heuristic optimization methods are more efficient than other optimization methods. For example, the other methods may not converge to local optimum, but heuristic methods do not need function derivatives, which means they have a great chance to find global optimum. Since heuristic methods do not require a derivative function, it is easy to apply to various optimization problems.

2.2 General Description of Genetic Algorithm

Philosophy of genetic algorithm is based on the adaptation mechanics of the most viable species. There is a direct correlation between this method and genetics in terms of terminology [8]. Holland [9] has established genetic algorithm in order to demonstrate the adaptive mechanism of natural systems. Genetic algorithm has distinct aspects that outperform the conventional optimization methods [10]. These aspects in the sense of advantages can be listed as follows:

- Parameters are coded as binary numbers in GA that present the effectiveness in the algorithm.
- The best solution is investigated around multiple points rather than a single point.
- The criterion of the optimization is based on the value of objective function, not function derivatives.
- Deterministic rules are not applicable in GA, since every operation is based on its probability.

2.2.1 Formulation of Optimization Problem in Genetic Algorithm

2.2.1.1 Design Variables (Genes)

Design variables are the numbers used in the optimization problem. These numbers have to be converted into a binary system. These binary numbers are called “genes”. Genes constitute a chromosome, in other words a string. According to the size optimization in truss problems, the design variables will be cross sectional areas (A_n):

$$X_n = (A_1, A_2, A_3, \dots, A_n) \quad (2.1)$$

where X_n is the vector of design variables in the algorithm [11].

Cross sectional areas represented above are genes, and three random genes are assigned to create a string such that:

$$String = A_1 A_2 A_3 \quad \quad \quad Binary\ code = 1111|1000|1100$$

2.2.1.2 Objective Function (Fitness)

General optimization problems are evaluated by an objective function; however the objective function is embedded into fitness in GA. Each string has their fitness values, which are calculated through fitness function [1]. The optimization problem can be either maximization

or minimization. If the problem has to be maximized, the fitness function [12] must be equal to the objective function such that:

$$fitness = \sum_{i=1}^n f(x_n) \quad (2.2)$$

If the problem has to be minimized, the objective function [1] must be altered in order to calculate fitness. In this case, the lowest possible design variables will give the highest fitness values such that:

$$fitness = \frac{1}{1 + \sum_{i=1}^n f(x_n)} \quad (2.3)$$

In both cases, the fitness function is aimed to be maximum in GA.

2.2.1.3 Constraints

In the optimization problems, there are several conditions that have to be satisfied, especially in structural optimization. For instance, in steel truss optimization it is important to select a proper cross sectional area that will meet with the design criteria such as tensile strength, compression strength and deflection. However, the method itself does not allow solving the constrained optimization problems [13]. This issue can be eliminated by a penalty function. By inserting constraints into a penalty function, the constrained optimization problem becomes an unconstrained optimization problem. The penalty function [14] is formulated such that it is based on stress violation of structural members:

$$p(x_n) = \max \left[\frac{|\sigma_i|}{|\sigma_a|} - 1, 0 \right] \quad (2.4)$$

where σ_i and σ_a are stress in member i and allowable stress, respectively. If there is no violation in the element stresses, penalty value will be 0; otherwise, it will be a positive integer and affect the fitness such that:

$$fitness = \begin{cases} f(x_n) & \text{if } -\sigma_a \leq \sigma_i \leq +\sigma_a \\ f(x_n) - p(x_n) & \text{otherwise} \end{cases} \quad (2.5)$$

The duty of the penalty function as it is stated above is to decrease the fitness of undesirable strings in order to lower their potential of being a solution for the optimization problem.

2.2.2 Operators in Genetic Algorithm

There are four operators in GA: initialization, selection, crossover and mutation.

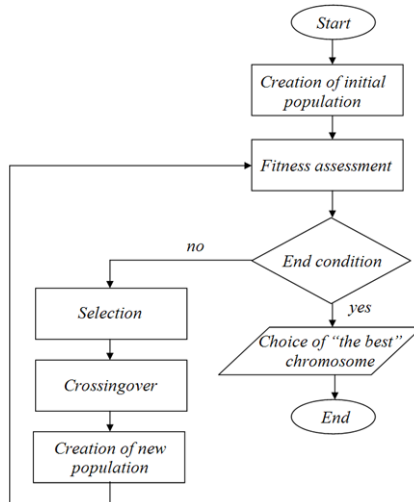


Figure 1: Genetic algorithm flow chart.

Genetic algorithm flow chart is shown in Figure 1. Genetic algorithm operators take place during the optimization. The end condition terminates the optimization when there is no more improvement in the population. The optimal solution (the best string) is chosen from the terminated population.

(a) Initialization

In genetic algorithm, searching for a solution begins from multiple points in the design domain [14]. Each point, namely strings, represents a possible solution for the problem. The population comprises of the strings, and the size of the population affects the computation time dramatically.

(b) Selection (Reproduction)

After initializing a population, the selection of the best individuals (strings) from the population is an essential part of the genetic algorithm. This operation involves the selection of strings based on their fitness values in the population. In other words, valuable strings have more chance to transfer descendants to the new generation [14]. As a selection method, roulette wheel selection is recommended by Holland [15]. In this method, a number of selections are equivalent to the population size in order to have same population size in the next generation. Selections are made according to the ratio between fitness value of one string and total fitness value of the whole population.

(c) Crossover

All selected strings according to roulette wheel selection are put into mating pool for crossover. Crossover operation is conducted in two phases. Firstly, new selected members

are mated to each other randomly in the mating pool. Secondly, each coupled string is crossed over at a location K through the string. K is a random integer that varies between 1 and string length less 1 ($1, L-1$) [10]. When the location K is set, all genes after position K will be switched along the coupled strings. The location K is illustrated with |.

For example:

Before Crossover	After Crossover
$A_1 = 01101 0$	$A'_1 = 011011$
$A_2 = 11001 1$	$A'_2 = 110010$

(d) Mutation

Mutation is a useful operator to keep diversity in the population with a small possibility [1].

Mutation alters a single gene 0 to 1 or 1 to 0 in the string.

For example:

Before Mutation	After Mutation
$A_1 = 00100$	$A'_1 = 10100$
$A_2 = 11001$	$A'_2 = 10001$

The first gene in A_1 and the second gene in A_2 have been mutated. This operator serves as a local enhancement while algorithm is working, and increases the speed of convergence to an optimal solution.

2.2.3 Parameters in Genetic Algorithm

There are three parameters in genetic algorithm: population size (P_{size}), crossover probability (P_c) and mutation probability (P_m). In structural optimization, population size (total individuals in each generation), crossover probability and mutation probability are recommended as 25-125, 0.6-0.9 and 0.005-0.05, respectively by Roman et al [14].

2.2.4 Optimization Examples Using Genetic Algorithm

Two different optimization examples will be presented in this section in order to demonstrate robustness of GA. MATLAB is used to develop the optimization problem. It is important to indicate that MATLAB always tries to minimize the objective function in GA toolbox. For this reason, if the optimization problem is desired to be maximized, the objective function has to be taken as the reciprocal.

2.2.4.1 Size Optimization of 10-Element Planar Truss

This problem is a benchmark for size optimization of truss structures which have been studied by Schmit and Farshi [16], Schmit and Miura [17], Venkayya [18], Sedaghati [19], Kaveh and Rahami [20], Li et al. [21], Farshi and Ziazi [22], Asl, Aslani and Pahani [23]. In this problem, the goal is to find minimum structural weight by changing the members' cross sectional areas. This problem has two design constraints such as member displacement ($u_a = +2in$) and stress ($\sigma_a = +25ksi$). Optimization is performed using MATLAB GA optimization toolbox.

MATLAB is very efficient for this kind of optimization problem, because it allows to merge finite element model of a truss into genetic algorithm. In this problem, population size is set to 200. In GA population size between 100 and 200 is recommended if the number of variables is higher than 5. Otherwise, population size less than 100 is sufficient for optimum solution. Table I shows material properties of the benchmark problem. The material properties do not represent any specific material, they are used consistently by the researchers mentioned above. The boundary conditions and the load configuration of the benchmark problem are shown in Figure 2.

TABLE I: Material properties of 10-element planar truss.

Modulus of Elasticity, E	10,000ksi
Density, ρ	0.1lb/in ³
u_a	$\pm 2in$
σ_a	$\pm 25ksi$

The objective function of this problem is defined as minimizing the total weight of the structure ($w = \sum_{i=1}^{10} \rho A_i l_i$) while the element stresses (σ_i) and displacements (u_i) are limited by σ_a and u_a , respectively.

The variables w , ρ , A_i , l_i , u_i , u_a , σ_i , σ_a are weight of the truss, density, member cross sectional area, member length, member displacement, allowable displacement and member stress

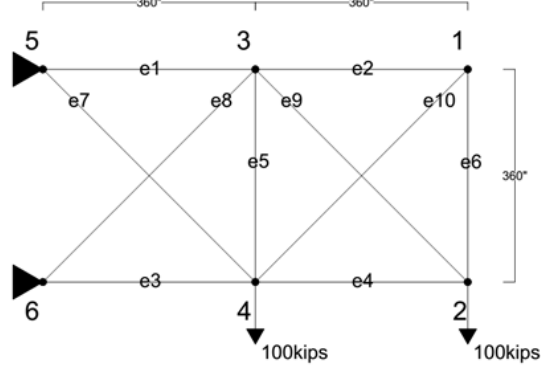


Figure 2: 10-element planar truss.

and allowable stress, respectively. The design domain is squeezed into $0.1in^2$ and $35in^2$ by assigning upper and lower bounds of member cross sectional areas.

TABLE II: Comparison of the weight minimization results.

Design Variables, in^2	Schmit and Farsh [16]	Venkayya [18]	Schmit and Muira [17]	Kaveh and Rahami [20]	Farshi and Ziazi [22]	Li et al. [21]	Sedaghati [19]	Asl et al. [23]	This Work
A_1	33.43	30.42	30.67	30.67	30.52	30.70	30.52	30.51	30.25
A_2	0.10	0.13	0.10	0.10	0.10	0.10	0.10	0.10	0.10
A_3	24.26	23.41	23.76	22.87	23.20	23.17	23.20	23.20	23.80
A_4	14.26	14.91	14.59	15.34	15.22	15.18	15.22	15.19	14.95
A_5	0.10	0.10	0.10	0.10	0.10	0.10	0.10	0.10	0.10
A_6	0.10	0.10	0.10	0.46	0.55	0.55	0.55	0.56	0.59
A_7	8.39	8.70	8.58	7.48	7.47	7.46	7.46	7.46	7.41
A_8	20.74	21.08	21.07	20.97	21.03	20.98	21.04	21.07	20.92
A_9	19.69	21.08	20.96	21.70	21.53	21.51	21.53	21.47	21.57
A_{10}	0.10	0.19	0.10	0.10	0.10	0.10	0.10	0.10	0.10
Total Weight, lb	5089.00	5084.90	5076.85	5061.90	5061.40	5060.92	5060.85	5058.66	5057.71

Table II presents the minimized total weight of the problem. According to the results, GA optimized the structure by achieving lighter weight than the other works.

2.2.4.2 Size Optimization of 10-Bay Periodic Truss Bridge

Size optimization of a 10-bay periodic truss bridge has a similar optimization process as the benchmark problem. All truss connections are pinned and the structural members are selected as bar elements. It is assumed that there are bridge piers at every 10-bay. The boundary conditions are assumed as simply supported at each end. While optimization is performed, tensile and buckling strength and vertical deflection at the mid span are taken into consideration as the constraints. Since the bridge is symmetrical along its deck, the bridge is modeled as 2D planar truss instead of 3D truss.

Every optimization has different solutions with respect to the loads applied on the system. In this study, the optimization has been done according to $4000psi$ concrete strength and live load of HS20 truck. AASHTO [24] states that distributed live load of HS20 truck is $53.33lb/in$ for each lane.

TABLE III: Total load for each bay of the truss.

Concrete Deck	$539.97kips$
HS20 Truck	$76.80kips$
Total	$616.76kips$

Table III shows the total dead and live load to which each bay of the system is exposed. Total load is distributed to each unit cell equally as shown in Figure 3.

Similar to the benchmark problem, minimization of the total weight ($w = \sum_{i=1}^{10} \rho A_i l_i$) is the objective function. The element tensile (T_i) and compression (C_i) stresses are constrained by yielding strength (σ_y) and buckling strength (C_n), respectively. The Deflection limit (u_a) is applied to node 6 alone, because it is at midspan. The algorithm finds optimum cross sectional areas of the bar elements between $1in^2$ and $75in^2$. The material properties of the truss bridge are given in Table IV.

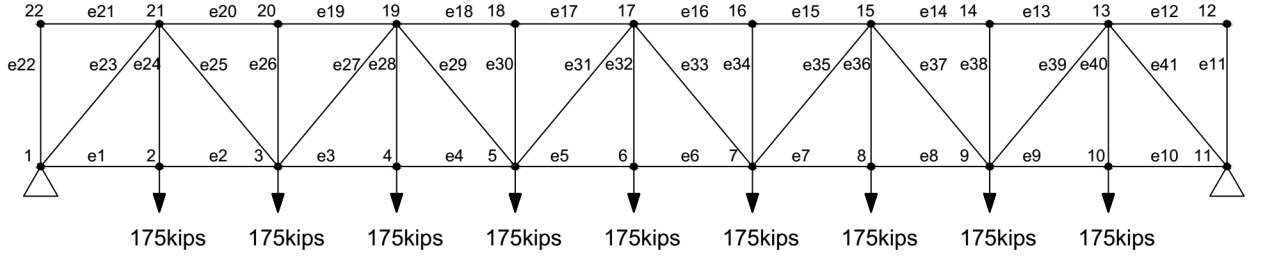


Figure 3: Load distribution along the truss, x-z view.

TABLE IV: Materials properties (ASTM A992 Steel).

Modulus of Elasticity, E	29,000ksi
Density, ρ	0.28b/in ³
u_a , $L/300$	6in
σ_y	50ksi

Buckling load, P_n is classified into two cases: elastic and inelastic buckling according to AISC 360-16 [25].

$$P_n = F_{cr} A_g \quad (2.6)$$

F_{cr} , the critical stress depends on:

$$F_{cr} = \left[0.658 \frac{F_y}{F_e} \right] F_y, \quad \text{if } \frac{KL}{r} \leq 4.71 \sqrt{\frac{E}{F_y}} \quad (2.7)$$

$$F_{cr} = 0.877 F_e, \quad \text{if } \frac{KL}{r} > 4.71 \sqrt{\frac{E}{F_y}} \quad (2.8)$$

where F_e , K , r and L are Euler buckling load, column effective length factor, radius of gyration, and member length, respectively. Since all structural members have pin connections, K is considered as 1. Similar to the previous problem, finite element analysis of the truss is embedded into GA as a constraint in MATLAB.

TABLE V: Weight minimization results of the truss.

Design Variables, in^2							
A_1	28.31	A_2	15.55	A_3	22.87	A_4	11.11
A_5	20.44	A_6	22.22	A_7	8.05	A_8	8.89
A_9	17.10	A_{10}	14.68	A_{11}	6.83	A_{12}	20.45
A_{13}	26.53	A_{14}	26.88	A_{15}	32.60	A_{16}	65.18
A_{17}	32.64	A_{18}	43.35	A_{19}	29.98	A_{20}	27.62
A_{21}	1.16	A_{22}	1.24	A_{23}	20.40	A_{24}	16.57
A_{25}	24.78	A_{26}	3.86	A_{27}	22.69	A_{28}	3.79
A_{29}	14.60	A_{30}	10.65	A_{31}	9.57	A_{32}	50.11
A_{33}	9.61	A_{34}	4.19	A_{35}	14.17	A_{36}	17.69
A_{37}	27.62	A_{38}	1.42	A_{39}	19.95	A_{40}	4.03
A_{41}	20.32						
Total Weight, lb				57713.10			

Table V shows the weight optimization results of the truss bridge. Genetic algorithm finds the minimum cross sectional areas according to demanding capacity of the elements. Since every element in the truss has different demand/capacity ratio, cross sectional areas of the elements vary all along the bridge. However, according to the periodic design, all unit cells need to have the same cross section as well as topology. In order to make NDE method proposed in this research (based on impulse response method) applicable to the truss, the periodicity has to be satisfied. Therefore, a damage in the structure becomes traceable.

TABLE VI: Weight minimization results of the truss.

Design Variables, in^2							
A_1	20.44	A_2	22.22	A_3	20.44	A_4	22.22
A_5	20.44	A_6	22.22	A_7	20.44	A_8	22.22
A_9	20.44	A_{10}	22.22	A_{11}	10.65	A_{12}	65.18
A_{13}	32.64	A_{14}	65.18	A_{15}	32.64	A_{16}	65.18
A_{17}	32.64	A_{18}	65.18	A_{19}	32.64	A_{20}	65.18
A_{21}	32.64	A_{22}	10.65	A_{23}	10.65	A_{24}	50.11
A_{25}	9.61	A_{26}	10.65	A_{27}	10.65	A_{28}	50.11
A_{29}	9.61	A_{30}	10.65	A_{31}	10.65	A_{32}	50.11
A_{33}	9.61	A_{34}	10.65	A_{35}	10.65	A_{36}	50.11
A_{37}	9.61	A_{38}	10.65	A_{39}	10.65	A_{40}	50.11
A_{41}	9.61						
Total Weight, lb				62394.00			

Table VI shows optimization results of the truss bridge with periodicity using the results presented in Table V. Elements numbered 17, 16, 5, 6, 30, 31, 32, 33 and 34 are used as a periodic pattern, because these elements have the highest demand/capacity ratio. Total weight of the structure increases 4680.90 lb when periodicity is applied to the system.

2.2.5 Summary

In this chapter, GA is applied to different optimization problems. The first impression is that the number of design variables and constraints have a significant effect in the convergence time. Two numerical examples indicate that when the structural complexity (number of elements, constraints, geometry etc.) increases, the convergence time to the optimal solution increases as well. The integration of periodic design into the finite element analysis enhances the performance of the algorithm, thus the optimal solution is achieved efficiently. For instance,

in the 10-bay truss bridge example, only one portion of the bridge between its two piers is modeled instead of the entire structure. This reduces the work load of the algorithm, thereby the optimum solution is found rapidly.

CHAPTER 3

IMPULSE RESPONSE METHOD TO PERIODICALLY ASSEMBLED TRUSSES

3.1 Introduction

While most truss configurations are non-redundant, the detectability of damage has not been considered as a design variable. The most common Structural Health Monitoring (SHM) methods implemented to truss structures are vibration monitoring [26], strain monitoring [27], and acoustic emission [28]. Typically, the damage detection method is formulated based on truss geometry and materials. This approach requires the development of calibration curves using experimental data, and depends on many variables (e.g., connection details, boundary conditions, configuration), which reduce the minimum detectable damage. In this research, an inverse approach is proposed such that the ideal structural configuration with periodic placement truss units is built with the known localized dispersion curve such that the influence of damage can be deduced using nondestructive evaluation methods such as impulse response without any calibration curves and independent from the boundary conditions. Recent studies show that the periodic assemblies of structures influence the propagation of elastic waves in certain frequency bands with strong attenuation characteristics [29]. The periodic structure design has been investigated by Brun et al. [30] in order to suppress high vibration of slender multi-girder steel bridges by adding lightweight periodic waveguide truss system with particular

non-vibration frequency range equivalent to frequencies causing high vibration in the original structure. In addition to changing vibration modes, the periodic design can introduce unique material properties. For instance, Grima et al. [31] developed two and three dimensional truss structures exhibiting negative compressibility, which causes structural compression under axial tensile load. Hutchinson and Fleck [32] combined the matrix method with Bloch's theorem to analyze the structural behavior of periodic pin-jointed trusses.

In this research, the influence of damage in a periodic steel truss is inspected in terms of acceleration response. Acceleration history of three different unit cells in the truss are analyzed under impulse excitation. Numerical and experimental studies have been conducted in order to validate this research. In the first stage, impulse response of different numbers of unit cells is investigated using finite element analysis (FEA). This investigation has a crucial role in order to determine how many unit cells are needed for desired periodic behavior. In the second stage, an numerical simulations under impulse excitation of the truss are done using COMSOL Multiphysics software. The simulation includes both pristine and damaged conditions of the truss. In the third stage, eight-bay steel truss is built in laboratory, and acceleration response of the truss is recorded in both pristine and damaged conditions. In the experimental setup, 4 kHz impulse hammer and accelerometer are used as exciter and receiver, respectively. There are two principal questions, which are intended to be answered;

- Is it possible to obtain acceptable periodic behavior with limited number of unit cells in a system?

- How does acceleration response change in the vicinity of a damaged element in a periodically assembled system?

3.2 Numerical Results

3.2.1 Influence of Number of Unit Cells in Periodicity

In periodic trusses, each unit cell of the truss has periodic boundary condition, which is based on the assumption that the truss has infinite number of unit cells. In this case, each unit cell in the truss has the same response under an excitation, because each cell becomes independent from boundary conditions. However in reality, truss systems are built with finite unit cells, for this reason the responses of three adjacent unit cells assembled by combining 5, 15, 30, and 100 unit cell trusses are studied. For consistent results, each truss system has unit cells with the same shape, topology and cross sectional area. The procedure is carried out for 3 different unit cell topologies. Impulse transmission model is performed in frequency domain using COMSOL Multiphysics software. As an excitation signal, real impulse data is used in the finite element model, which is obtained from the impulse hammer. The frequency and time domain histories of impulse excitation are shown in Figure 5. The acceleration history of a selected node in a unit cell in -x direction is extracted from FEM. Figure 4 shows the excitation and measurement locations in the truss for three different topologies.

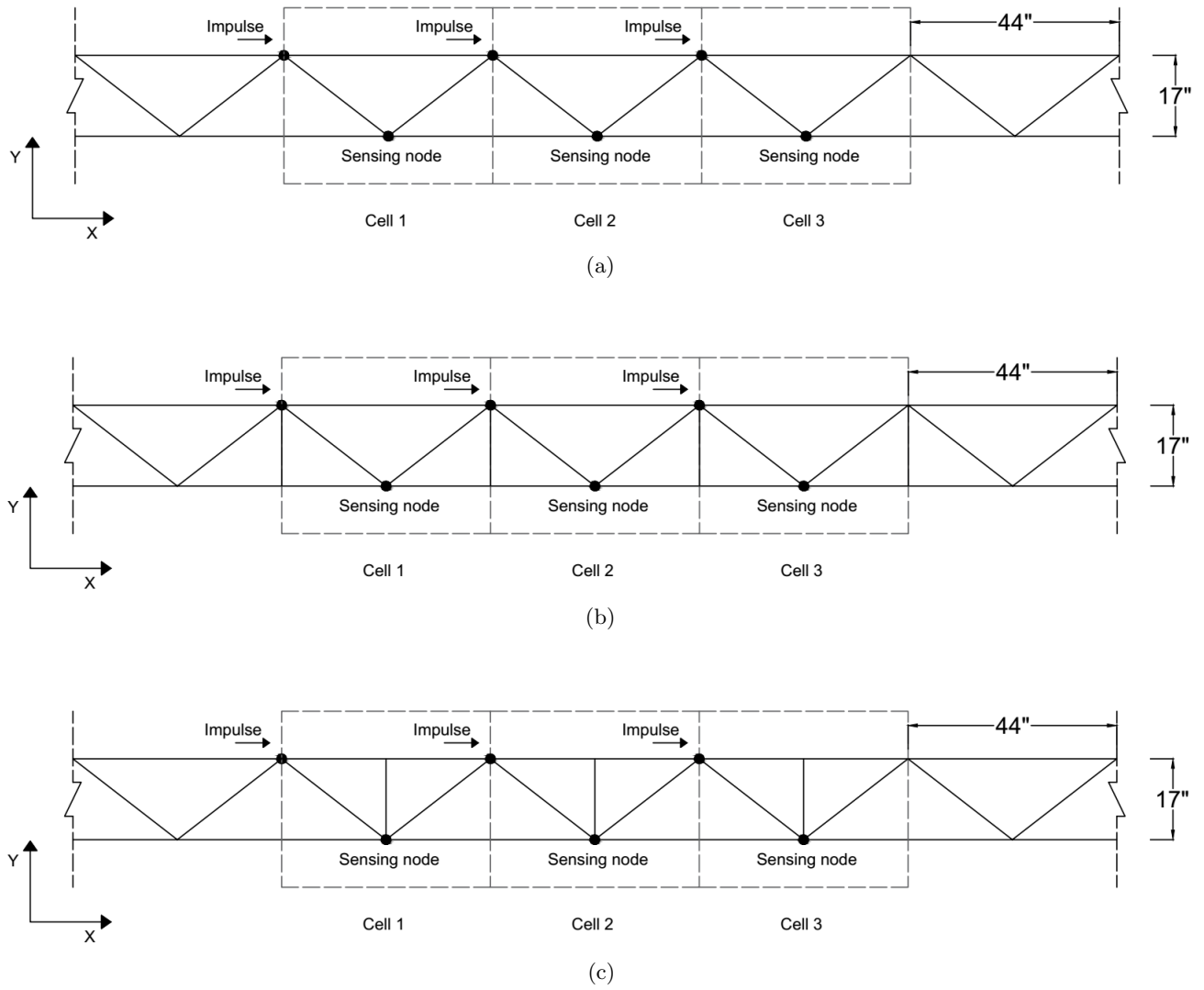


Figure 4: Different periodic assemblies of unit cells; (a) topology 1, (b) topology 2, (c) topology 3.

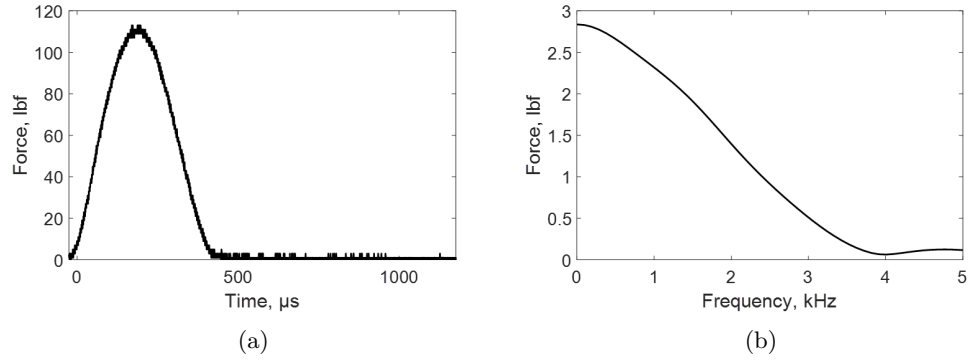


Figure 5: The impulse source using the impact hammer; (a) time domain, (b) frequency domain.

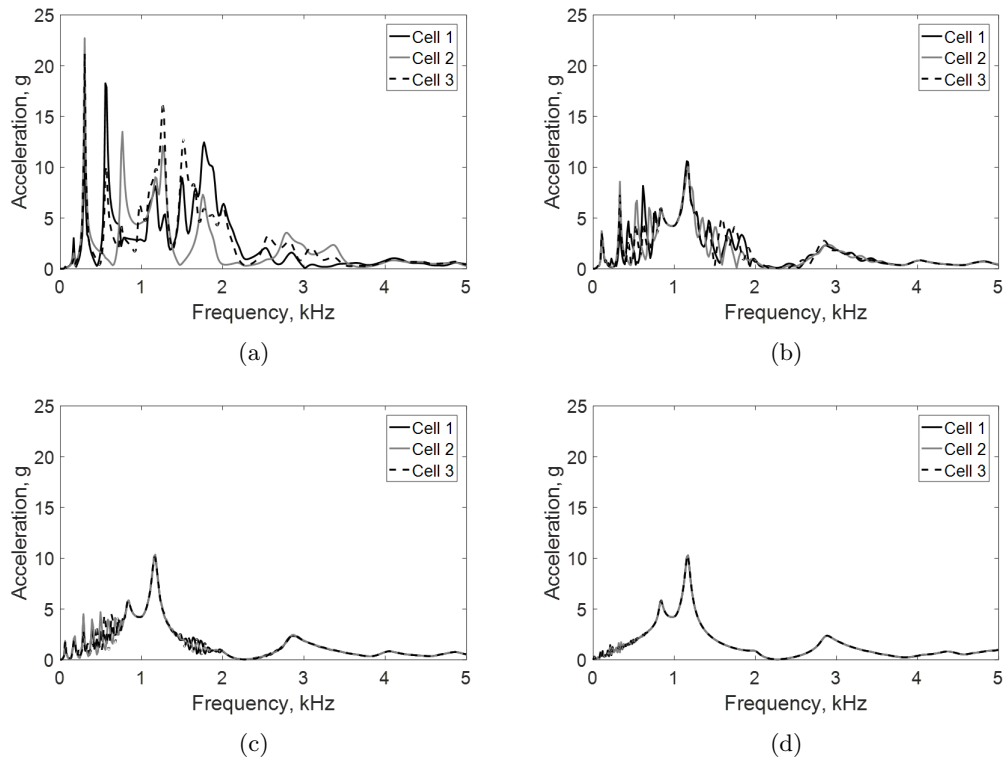


Figure 6: Impulse response of truss topology 1; (a) 5 cells, (b) 15 cells, (c) 30 cells, (d) 100 cells.

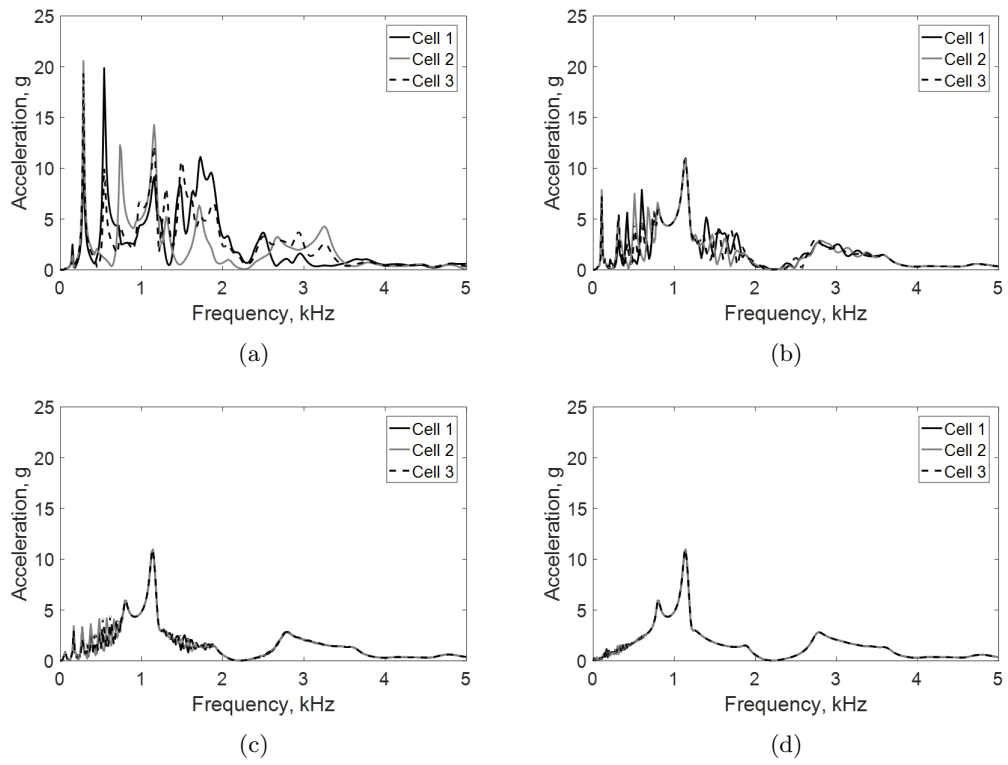


Figure 7: Impulse response of truss topology 2; (a) 5 cells, (b) 15 cells, (c) 30 cells, (d) 100 cells.

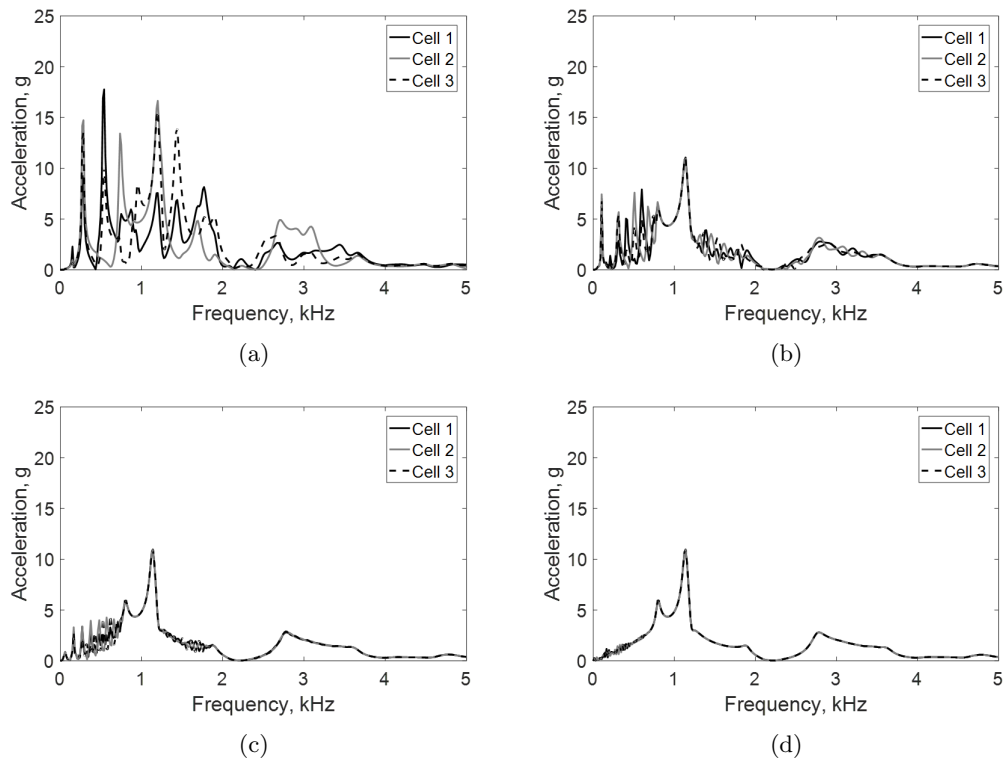


Figure 8: Impulse response of truss topology 3; (a) 5 cells, (b) 15 cells, (c) 30 cells, (d) 100 cells.

Figures 6, 7 and 8 show that the periodic behavior of a truss system is directly proportional to number of finite unit cells. However, there is no dissimilarity between three different topologies in terms of their impulse responses as the arrangements of truss members in the horizontal (periodic) direction are similar. By considering this, topology 1 is used building the experimental truss model. The truss model with 8 unit cells is selected in order to observe the periodic behavior experimentally with finite number of unit cells.

3.2.2 Experimental Truss Configuration

Finite element model of 2D truss consists of 35 circular hollow section steel bars built originally by ASCE students for bridge competition. The truss system is simply supported at both ends, and each bars is considered as pin connection. 5% damping is assumed in the finite element model. Boundary conditions, dimensions, impulse and sensor locations are presented in Figure 9. This configuration is used in both experimental and numerical models. Table VII shows the material properties and cross sectional areas of the truss elements.

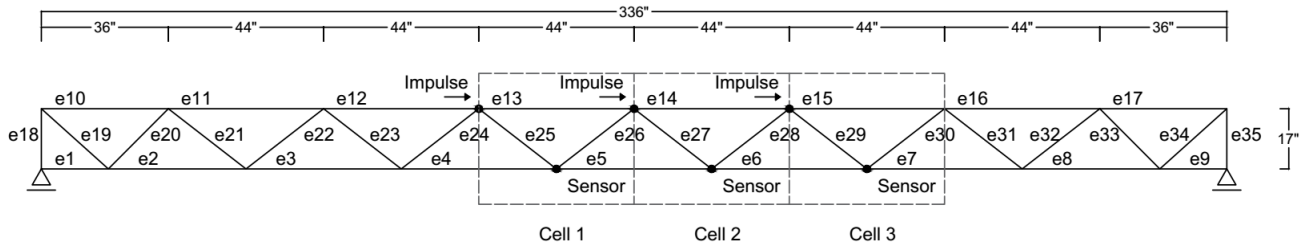


Figure 9: Truss configuration.

TABLE VII: Material properties and cross sectional areas of the bar elements.

Material Properties		Cross sectional Area, in^2	
Density, ρ	$490lb/ft^3$	e_1, e_9	0.17
Modulus of Elasticity, E	$29000ksi$	e_{18}, e_{35}	0.76
Poisson's Ratio, ν	0.33	e_2-e_{34}	0.23

3.2.3 Impulse Response of 2D Truss Using COMSOL Multiphysics Software

Transmission model is performed using COMSOL Multiphysics software for both pristine and damaged conditions.

3.2.3.1 Pristine Condition

The impulse responses of three adjacent unit cells with the pristine condition are shown in Figure 10. The first two peak frequencies at 0.18 kHz and 1.18 kHz agree with each other. The periodic behavior is observed better after 4 kHz as the influence of boundary condition reduces at higher frequencies.

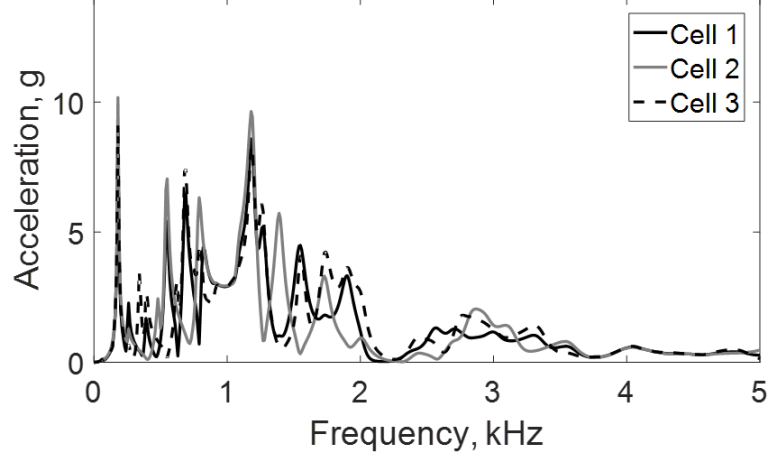


Figure 10: Numerical impulse responses of three adjacent unit cells for the pristine truss.

3.2.3.2 Damaged Condition

The influence of damage in elements e_{25} , e_{27} and e_{29} is studied separately. In the experimental model, damage is introduced by 50% cross sectional area reduction using saw cut in a bar element, and replaced separately for e_{25} , e_{27} and e_{29} . The damage in the finite element model is introduced as stiffness reduction. The equivalent stiffness reduction due to local area change needs to be calculated. The local element stiffness matrix for 2D bar is:

$$[k] = \frac{AE}{L} \begin{bmatrix} C^2 & CS & -C^2 & -CS \\ CS & S^2 & -CS & -S^2 \\ -C^2 & -CS & C^2 & CS \\ -CS & -S^2 & CS & S^2 \end{bmatrix} \quad (3.1)$$

where k is local element stiffness matrix, A is cross sectional area, E is Modulus of Elasticity, L is element length, C and S are cosine and sine with respect to global axis of the bar element [33]. Cross sectional area of the bar elements controls the stiffness. In order to find equivalent stiffness reduction due to 50% cross sectional area reduction at a local point, 3D solid models of pristine and damaged bar elements are configured. For linear and elastic systems, nodal forces are calculated by

$$\{F\} = [K] \cdot \{d\} \quad (3.2)$$

where F is the vector of global nodal forces, d is the vector of displacements, and K is the global stiffness matrix [33]. The stiffness reduction in 3D model can be found by applying axial unit force to the pristine and damaged models.

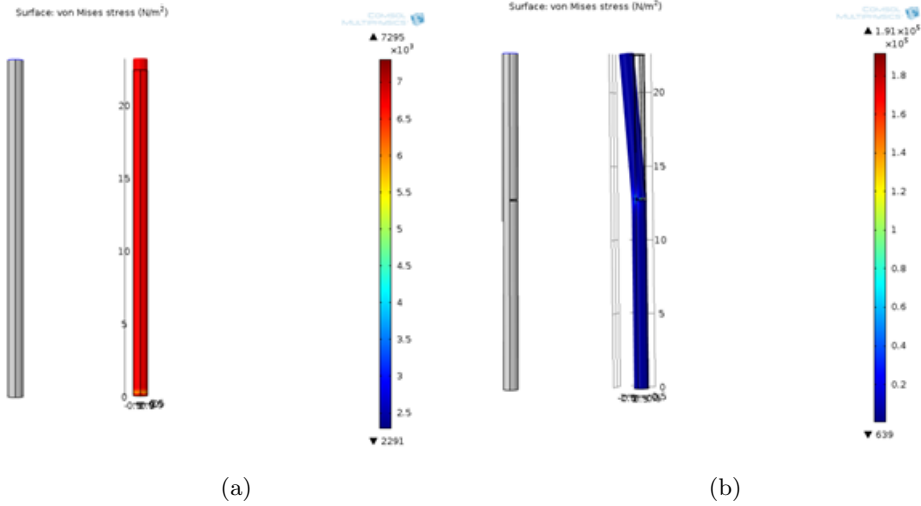
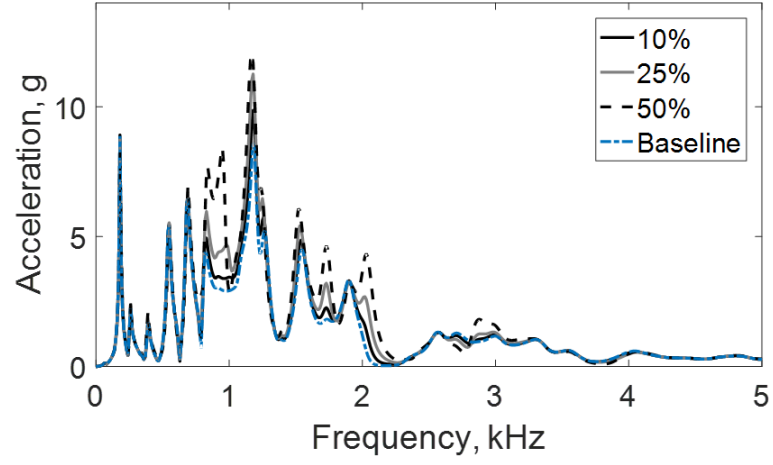


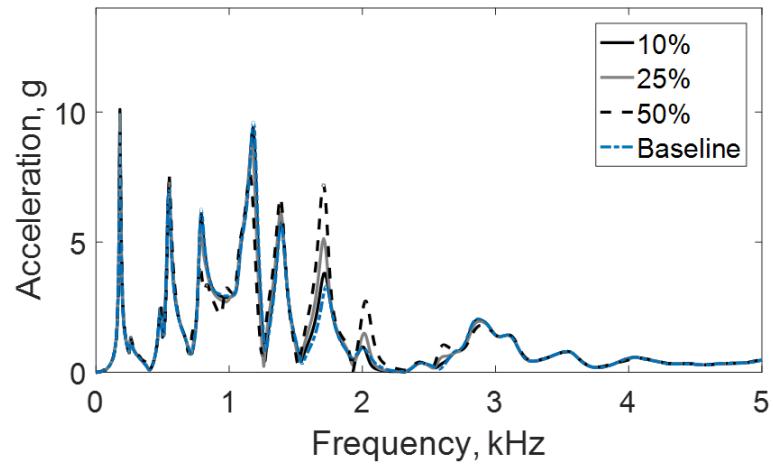
Figure 11: 3D solid models of damaged elements; (a) pristine, (b) damaged.

Figure 11 shows 3D models of a bar element for pristine and damaged conditions. Fixed boundary condition is assigned to the bottom of the bar element, and 1N unit force is applied to the top of the element in order to find the flexibility and then stiffness. According to the results from the 3D model of a damaged bar element, 50% local cross sectional area reduction causes 25% general stiffness reduction. For this reason, in order to compare numerical model and experimental model, 25% area reduction is constituted in the 2D finite element truss model in COMSOL Multiphysics software. Additionally, 10% and 50% reduced stiffness models are studied.

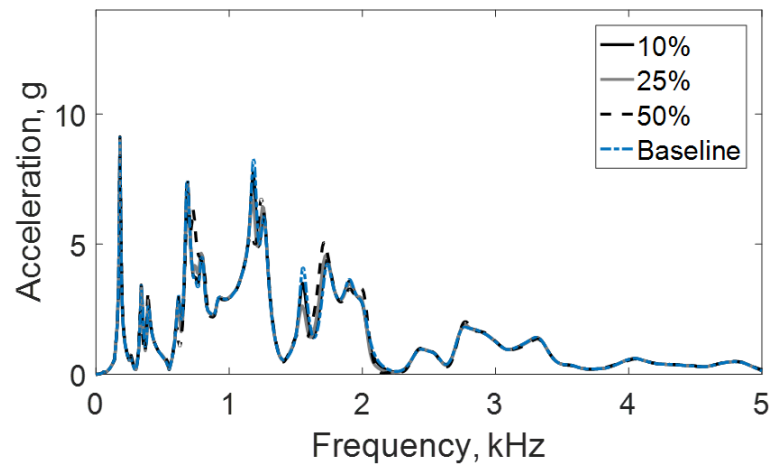
Figures 12, 13 and 14 show that the damage in the unit cells increases the acceleration response. This consequence has a good agreement with Eq. (3.2), because the excitation force is same for any measurement, and there is an inverse proportion between stiffness and displacement (response). The damaged unit cells have higher acceleration response than the other pristine cells, therefore damaged unit cells can easily be identified.



(a)

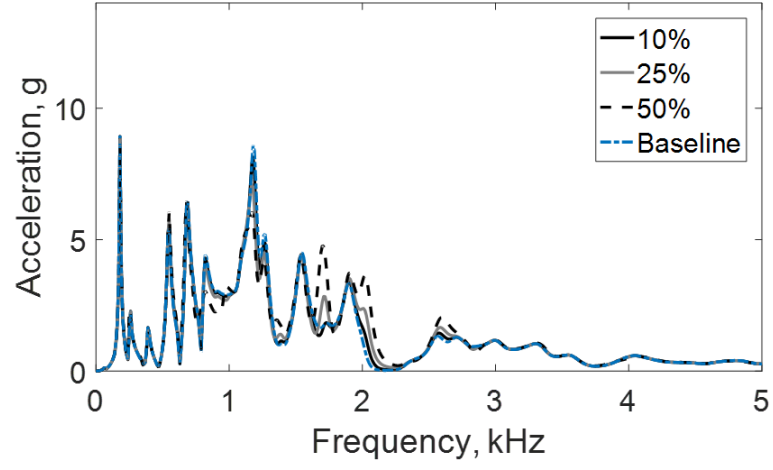


(b)

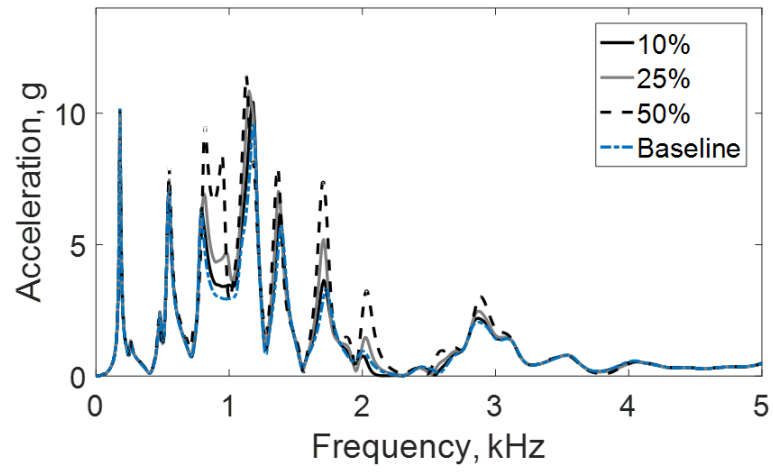


(c)

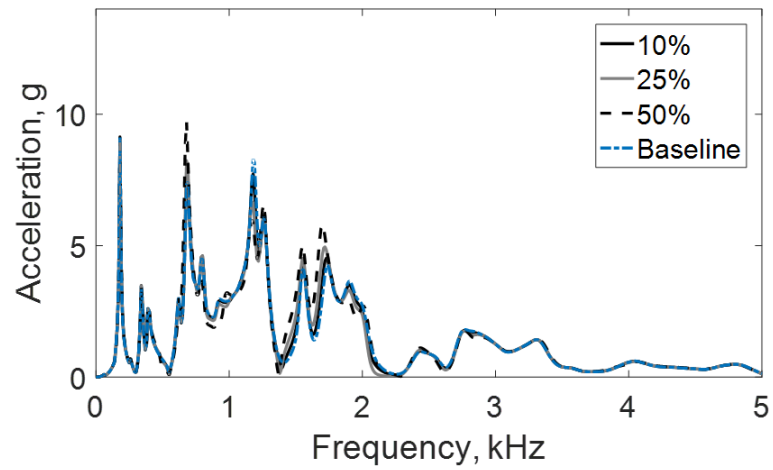
Figure 12: Numerical impulse responses when damage is introduced to member in unit cell 1; (a) unit cell 1 response, (b) unit cell 2 response, (c) unit cell 3 response.



(a)

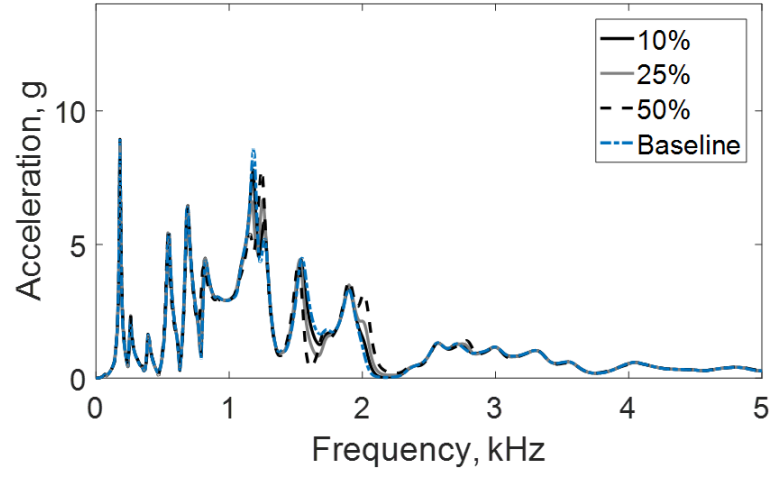


(b)

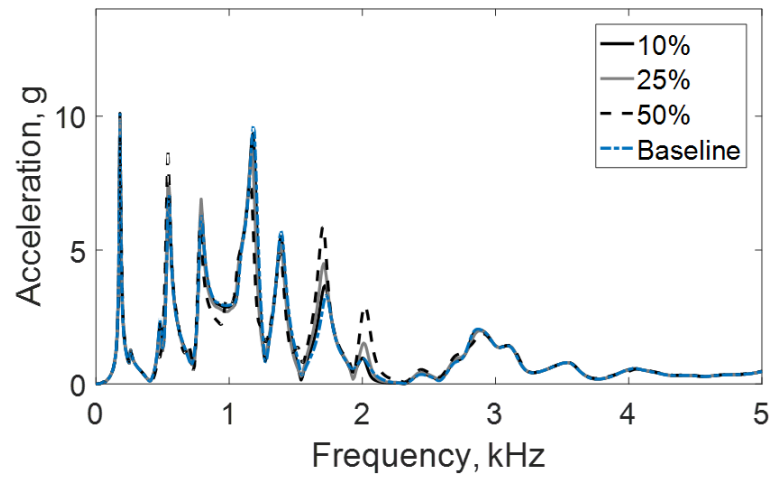


(c)

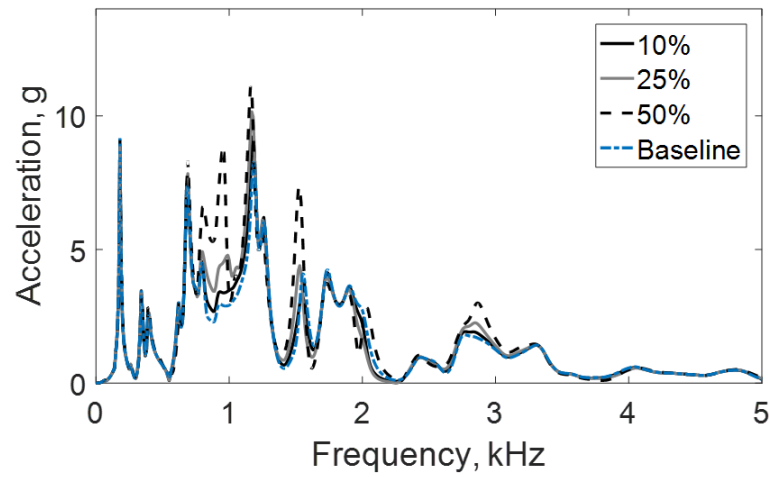
Figure 13: Numerical impulse responses when damage is introduced to member in unit cell 2; (a) unit cell 1 response, (b) unit cell 2 response, (c) unit cell 3 response.



(a)



(b)



(c)

Figure 14: Numerical impulse responses when damage is introduced to member in unit cell 3; (a) unit cell 1 response, (b) unit cell 2 response, (c) unit cell 3 response.

3.3 Experimental Results

3.3.1 Experimental Setup

The experimental setup has four major components: impulse hammer, uniaxial accelerometer, signal conditioner, oscilloscope and steel truss as shown in Figure 15. The impulse hammer (item no: 086C03) is manufactured by PCB PIEZOTRONICS with a variable tip to control the impact source function amplitude and duration. The impulse hammer has $10^{-2}V/lbf$ sensitivity. Uniaxial accelerometer (item no: 352C33) manufactured by PCB PIEZOTRONICS has the frequency bandwidth of 0.5-10000 Hz and sensitivity of $102.5 \times 10^{-3}V/g$. Both impulse hammer and accelerometer are connected to signal conditioner unit (item no: 482C05). The output of impulse hammer is connected to the first channel of oscilloscope to record the impulse source function and trigger the accelerometer. The impulse hammer is applied horizontally at each excitation location. The accelerometer attached horizontally to the truss system is connected to the second channel of the oscilloscope with 12.5 MHz sampling frequency and 10 ms duration.

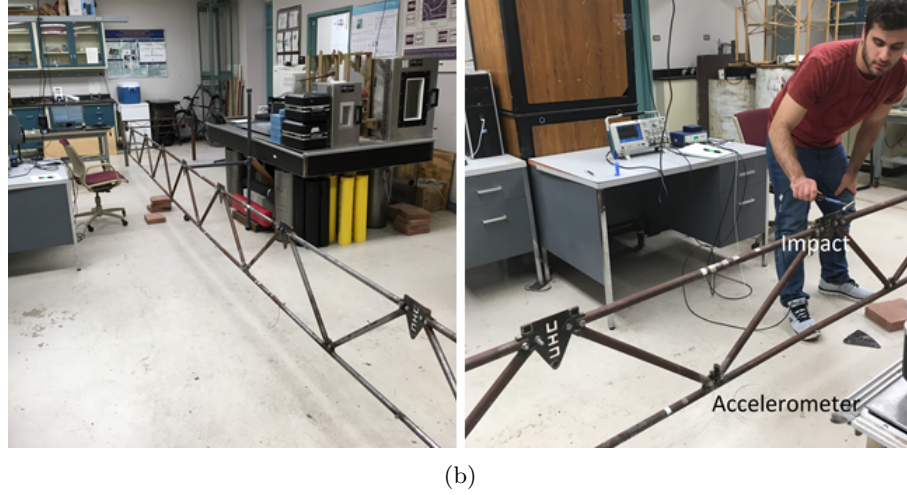
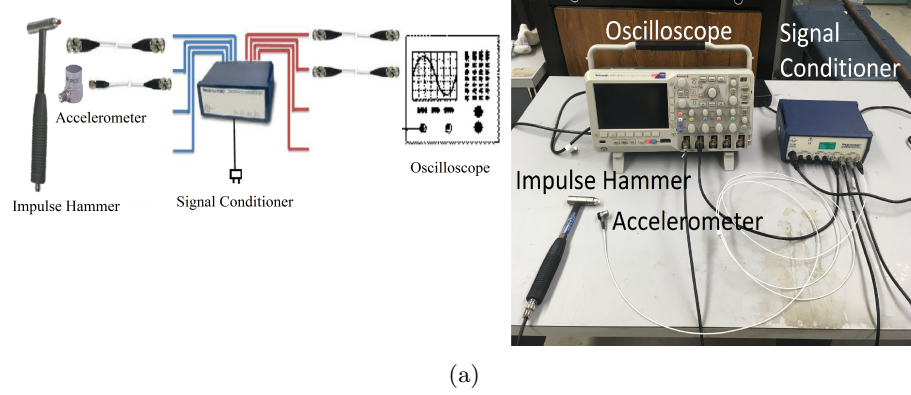


Figure 15: Experimental setup; (a) connection detail of the equipment, (b) bridge model.

3.3.2 Pristine Condition

The impulse response experiments are repeated five times for each unit cell. The locations of impulse hammer and accelerometer are moved as shown in Figure 9 for measuring the responses of each unit cell. Figure 16 and Figure 17 show time domain histories and their frequency spectra, respectively. The experiments show good repeatability. Figure 16 (d) and Figure 17 (d)

show the comparison of the averaged measurement of each unit cell in time domain and frequency domain, respectively. In general, the acceleration amplitudes and frequency distribution have similar behavior for all the unit cells for the pristine condition.

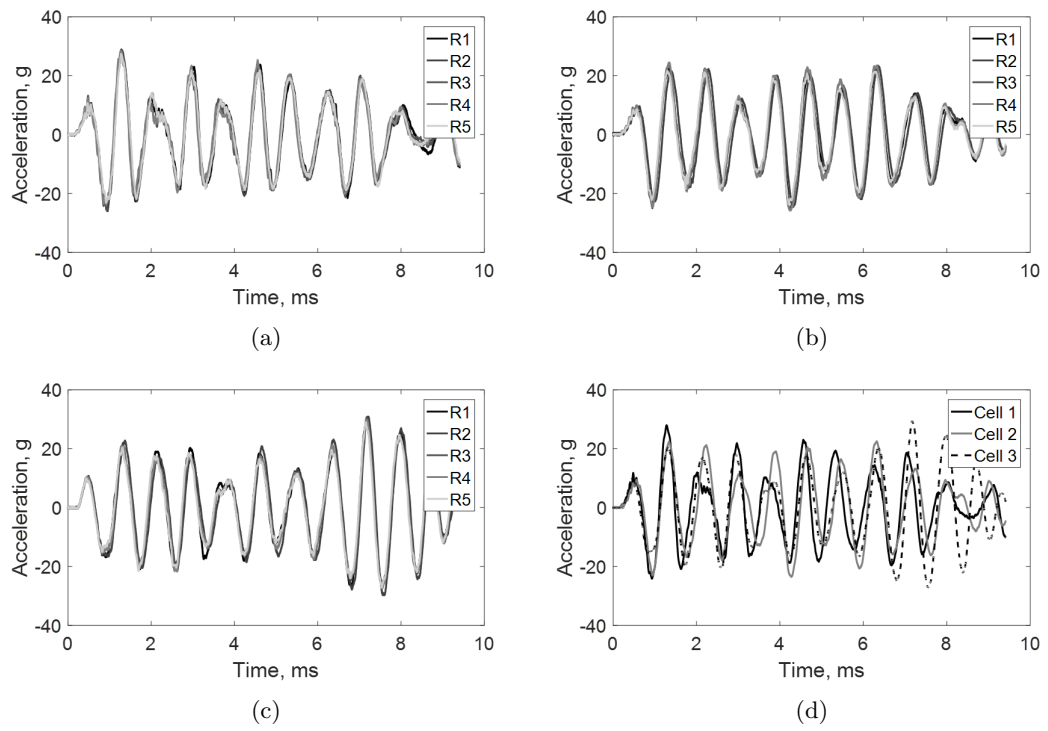


Figure 16: Time histories of the repeated impulse response results for; (a) cell 1, (b) cell 2, (c) cell 3, (d) the comparison of averaged waveforms of each unit cell.

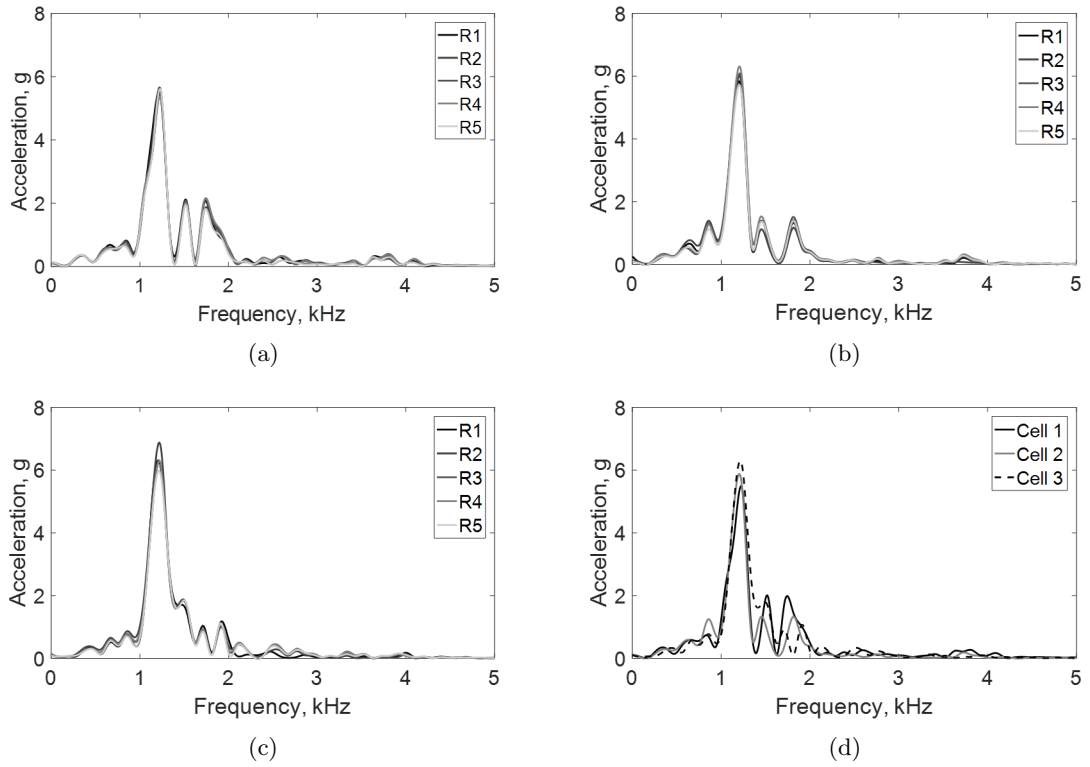
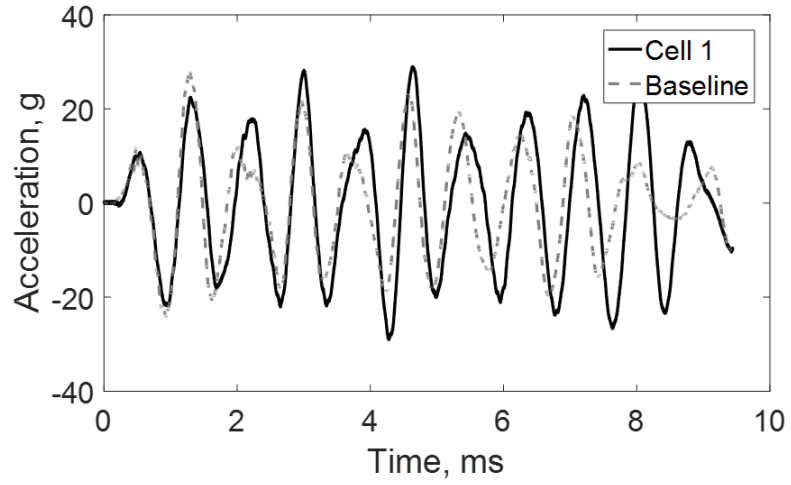


Figure 17: Frequency spectra of the repeated impulse response results; (a) cell 1, (b) cell 2, (c) cell 3, (d) the comparison of averaged frequency spectra of each unit cell.

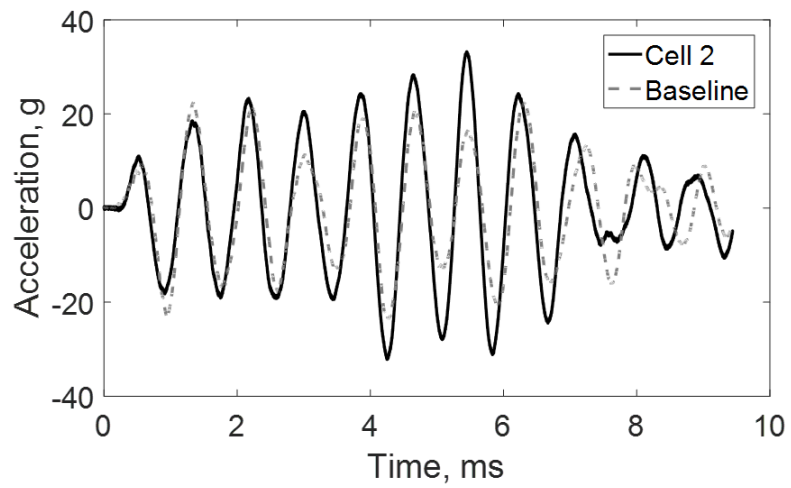
3.3.3 Damaged Condition

The damage is introduced sequentially in the three adjacent unit cell. The impulse responses of the unit cells have been measured in order to track the damage location. During the experiment, damage is proposed in unit cell 1, and the other unit cells are kept as pristine condition. The same procedure is performed for the other unit cells, thus the location effect of the damage can be observed.

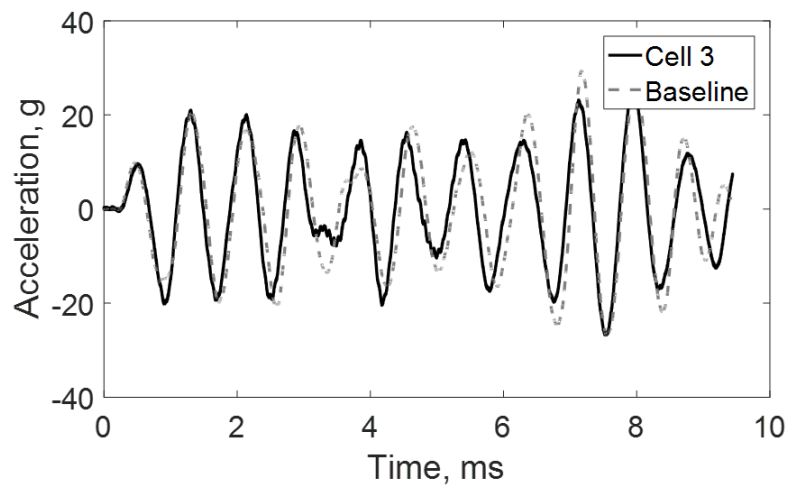
The numerical results are shown in Figures 18 to 23 in time and frequency domain. The results includes vibration responses of unit cells when damage is introduced sequentially to elements e_{25} , e_{27} and e_{29} . The damaged conditions of e_{25} (cell 1) and e_{27} (cell 2) cause significant increase at peak frequency amplitude when the damaged member is introduced into unit cell 1 or 2 while the response of unit cell 3 is similar to the pristine condition. When the damaged member is introduced into unit cell 3, it is noticed that all the unit cells diverge from the pristine condition. It is interpreted that the close proximity of unit cell 3 may cause such result.



(a)

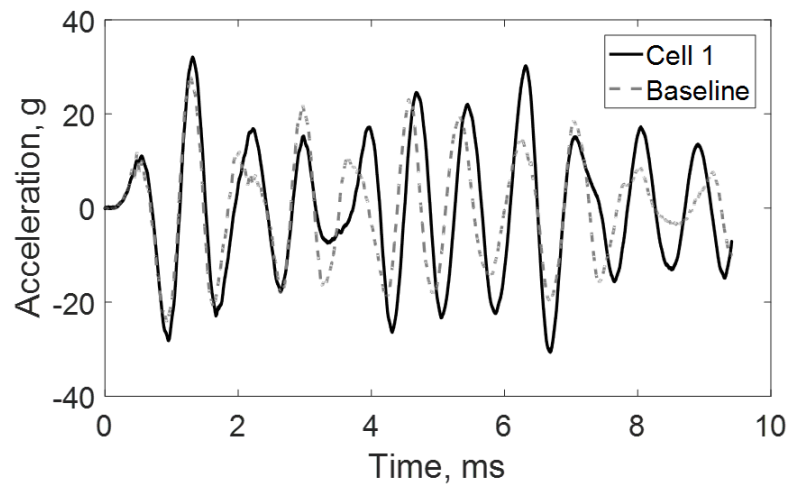


(b)

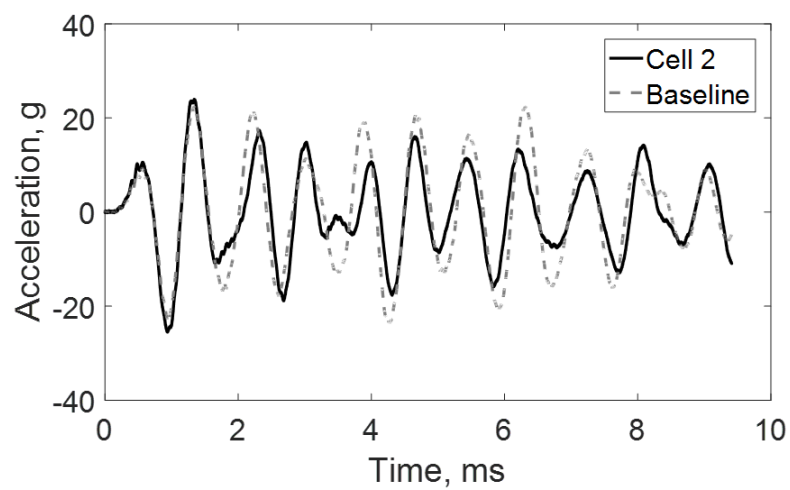


(c)

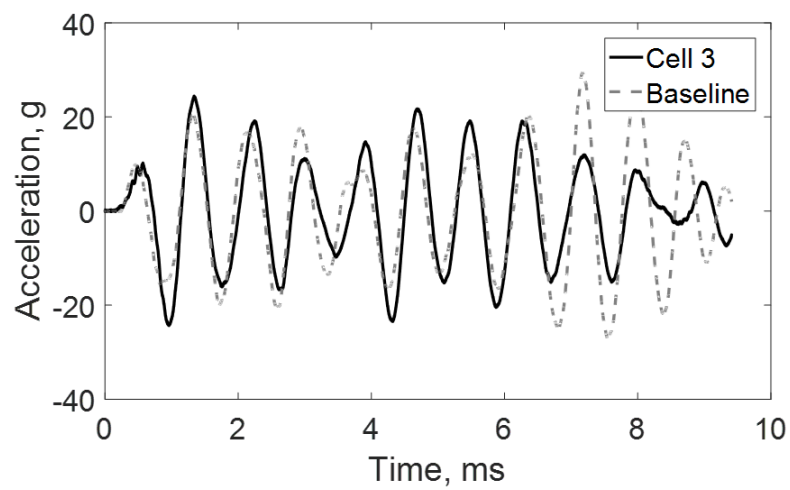
Figure 18: Time histories of three unit cells when damage member is introduced in cell 1; (a) cell 1, (b) cell 2, (c) cell 3.



(a)

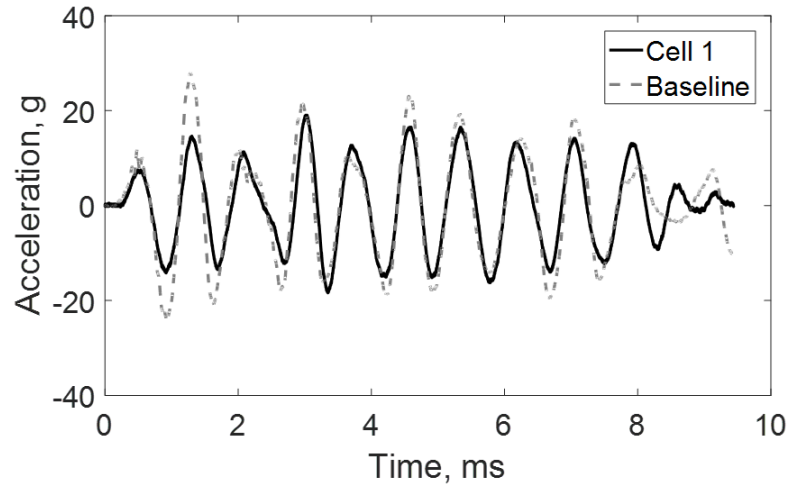


(b)

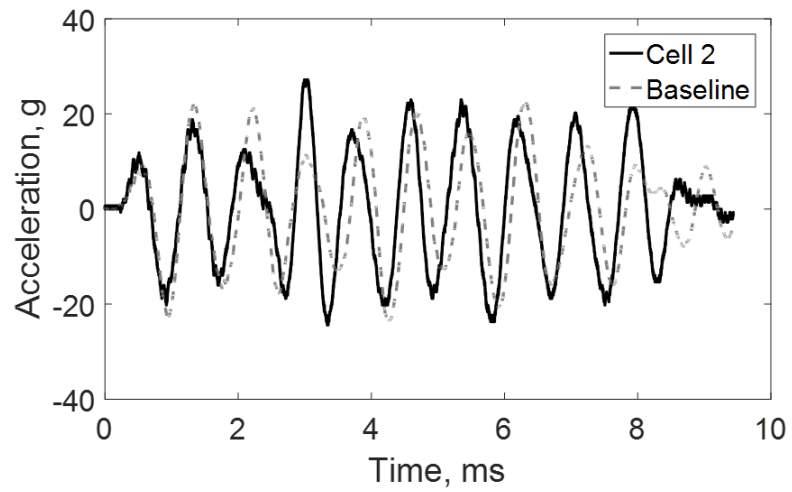


(c)

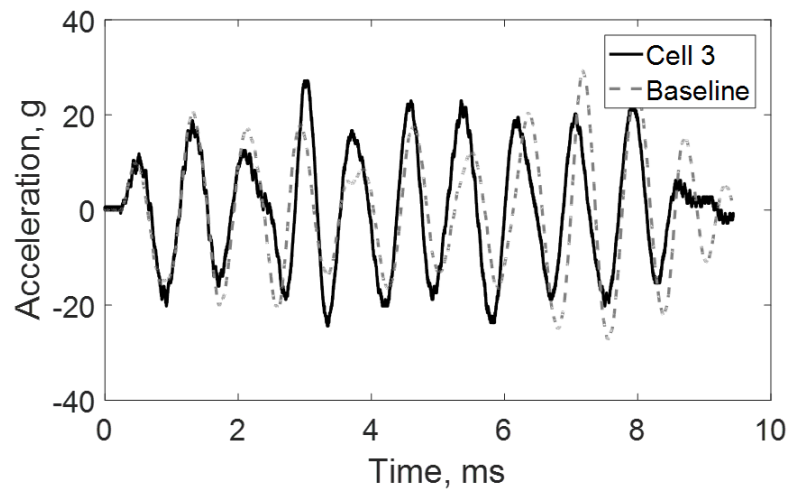
Figure 19: Time histories of three unit cells when damage member is introduced in cell 2; (a) cell 1, (b) cell 2, (c) cell 3.



(a)

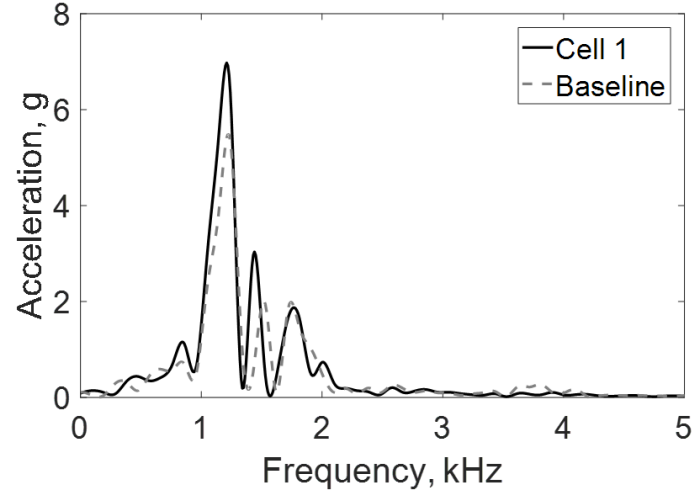


(b)

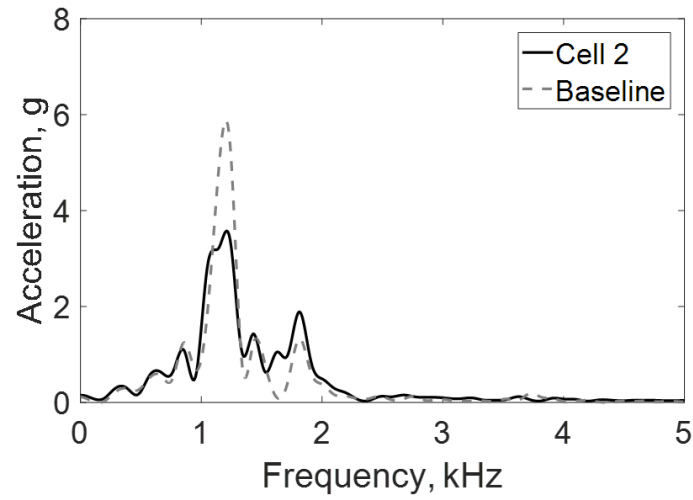


(c)

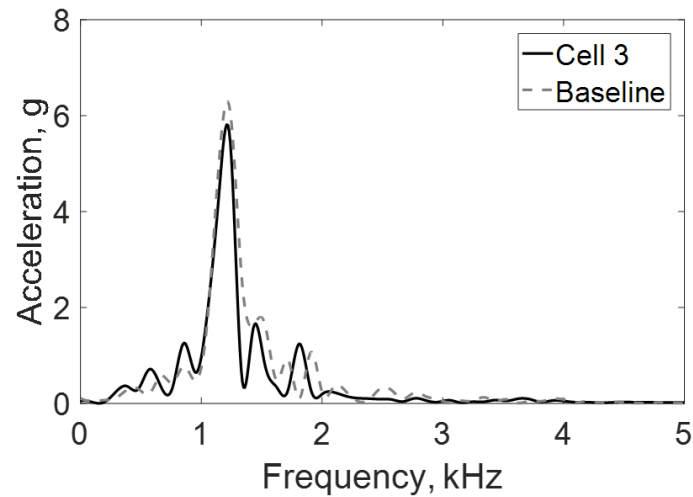
Figure 20: Time histories of three unit cells when damage member is introduced in cell 3; (a) cell 1, (b) cell 2, (c) cell 3.



(a)

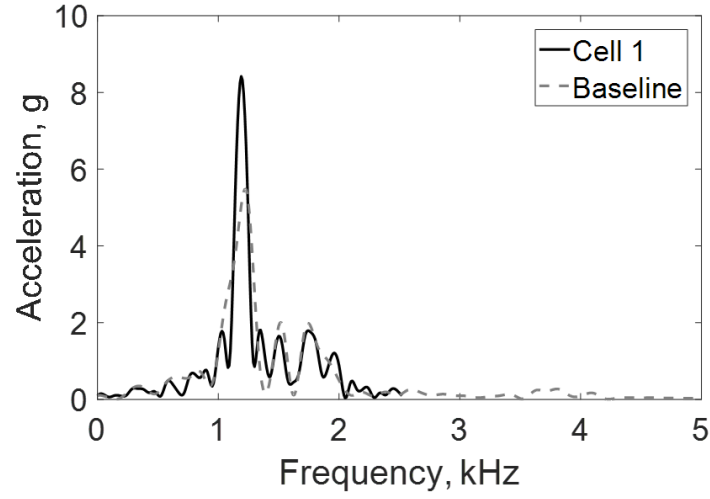


(b)

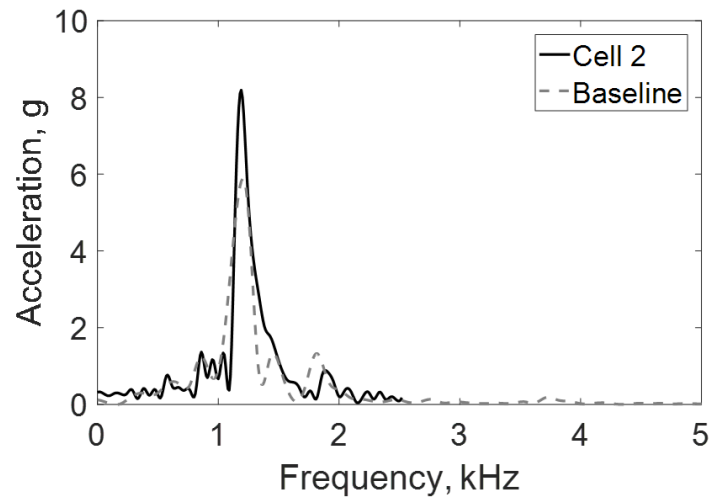


(c)

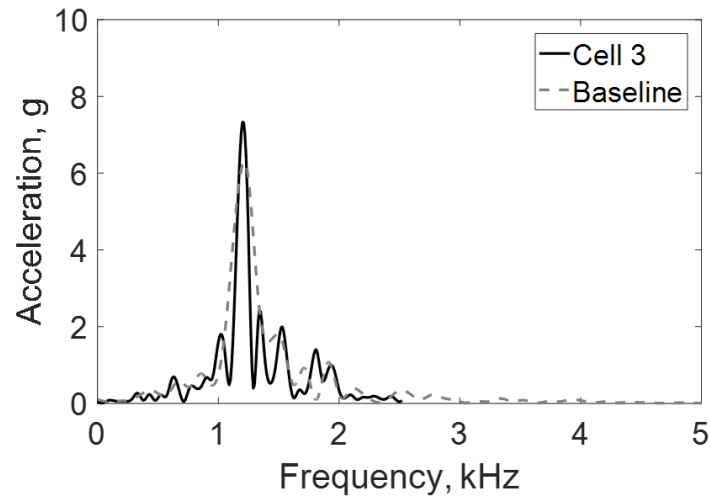
Figure 21: FFT results of five different impulse response of three adjacent unit cells when damage member is introduced in cell 1; (a) cell 1, (b) cell 2, (c) cell 3.



(a)

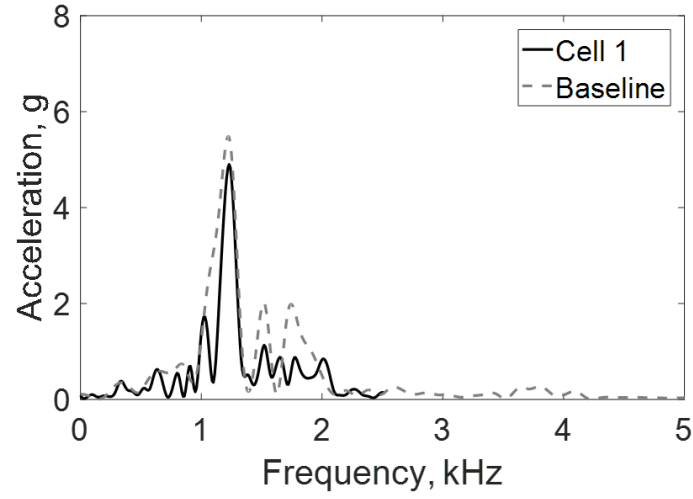


(b)

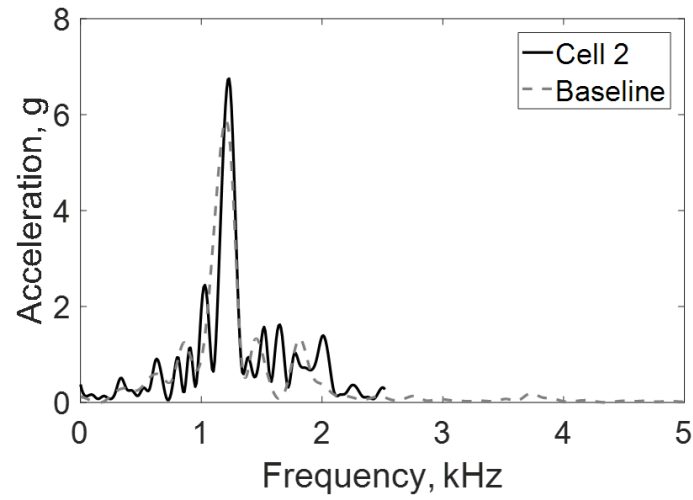


(c)

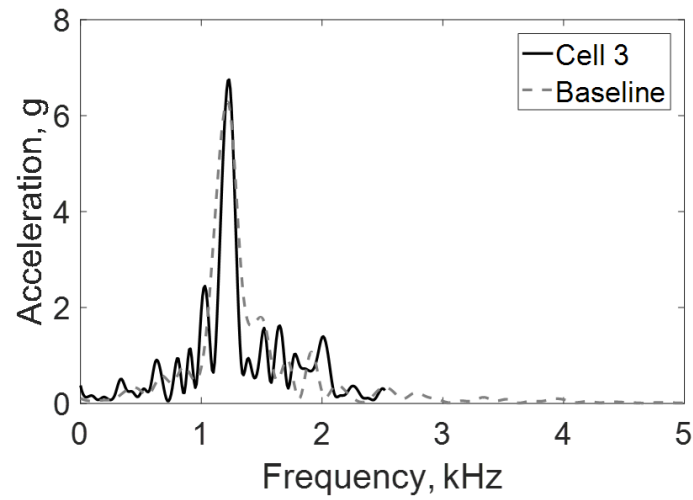
Figure 22: FFT results of five different impulse response of three adjacent unit cells when damage member is introduced in cell 2; (a) cell 1, (b) cell 2, (c) cell 3.



(a)



(b)



(c)

Figure 23: FFT results of five different impulse response of three adjacent unit cells when damage member is introduced in cell 3; (a) cell 1, (b) cell 2, (c) cell 3.

3.3.4 Calculation of Damping Using Q Factor Method

In the numerical model, 5% damping is assumed. Damping of the truss is calculated in order to validate the value used in numerical models. Q factor method is chosen as a tool for damping calculation. In the method, acceleration response of cell 2 pristine condition is used. Figure 24 shows the vibration response of cell 2 in using dB scale.

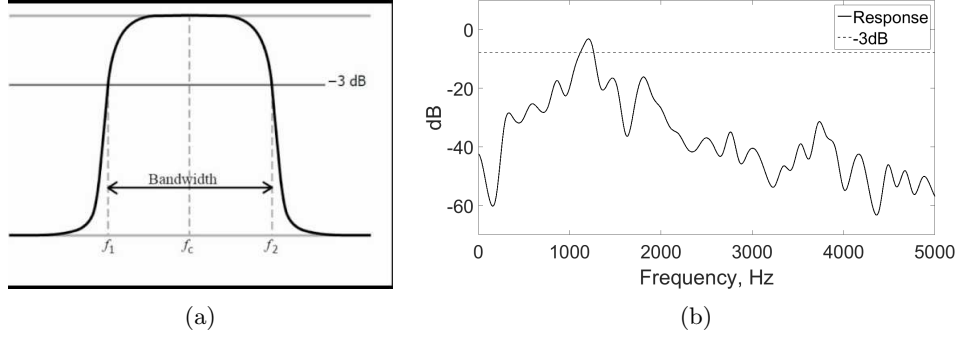


Figure 24: Q factor method; (a) notation, (b) cell 2 response in dB scale.

$$\xi = \frac{f_2 - f_1}{2f_c} \quad (3.3)$$

In Eq. (3.3) ξ is damping ratio, f_c is resonant frequency and $f_2 - f_1$ is half-power bandwidth [34]. According to calculations, damping is found as 6%. Since the actual damping of the truss is close to the assumed damping, numerical model is acceptable.

3.3.5 Comparison between Numerical and Experimental Results

The comparison between numerical and experimental models is performed by evaluating the peak energy of the resonant frequency in the acceleration response. Peak energy ratios for 25% stiffness reduction are given for both numerical and experimental models. In addition, numerical model includes peak energies between 10-50% stiffness reductions.

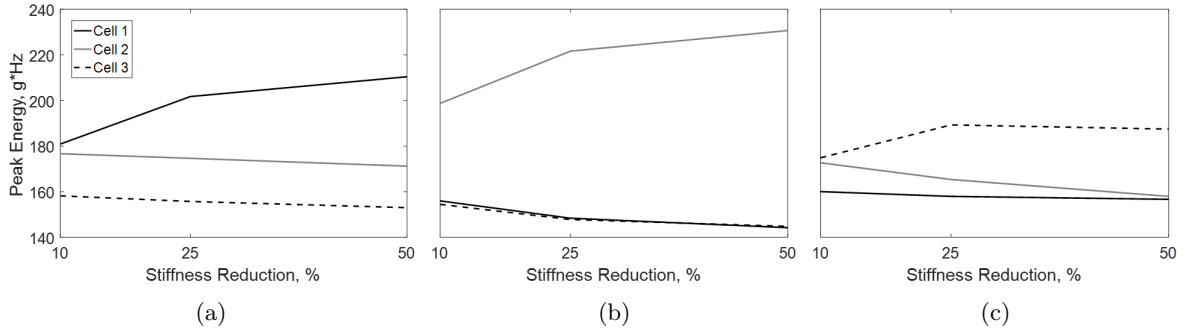


Figure 25: Peak energies for 10-50% stiffness reductions in numerical model; (a) damage in unit cell 1, (b) damage in unit cell 2, (c) damage in unit cell 3.

Figure 25 shows the peak energy levels for different stiffness reductions of numerical models which includes the damage cases in cell 1, 2 and 3. Since the vibration response increases proportionally for the increment of the damage, the peak energies also increases. According to Figure 25, the damaged unit cells have higher peak energies than other pristine unit cells. For this reason the damaged unit cells are identified explicitly.

TABLE VIII: Peak energy ratio comparison between numerical and experimental model for 25% stiffness reduction.

Numerical Model		Experimental Model
Damage in Cell 1	25%	23%
Damage in Cell 2	25%	16%
Damage in Cell 3	18%	-23%

The peak energy levels of numerical and experimental models for 25% stiffness reduction are compared in Table VIII. Both models have similar level of increase in terms of peak energy for cell 1 and cell 2 damage cases. However, the damaged conditions of experimental model in the unit cells 3 has lower increase than the numerical model. The reason for this can be due to inadequate bolt tensioning between experiments. Additionally, the unit cell 3 is close to the right end of the truss system, where boundary conditions may affect the system periodic behavior.

3.4 Summary

The acceleration responses of periodic trusses are studied using impulse response method numerically and experimentally. In the numerical models, the acceleration responses of three adjacent unit cell are evaluated for assembling 5, 15, 30 and 100 unit cell trusses. The evaluations show that the periodicity of the truss response is more apparent for high number of repetitive unit cells such as 100 unit cells. Additionally, periodicity is still applicable for a limited number of unit cells by considering the response near resonant frequency or higher frequency bandwidths.

The numerical and experimental models of a specific truss topology assembled with 8 unit cells are studied for pristine and damaged conditions. According to the results, the impulse response method allows to identify the location of the damage by evaluating the peak energy ratio levels of different unit cells.

CHAPTER 4

CONCLUSIONS

4.1 Summary

Genetic algorithm is a powerful tool for structural optimization. Size optimization of periodically assembled truss is performed using genetic algorithm. The periodicity of the system is ensured before and after the optimization for combining with the NDE method of impulse response. Implementing the periodicity of the system into the optimization not only provides an efficient optimization, but also gives better understanding about the structural behavior. The objective of this thesis is to develop an inverse method by including both structural optimization and NDE into the same platform.

Genetic algorithm optimization is applied to two different truss systems. The first optimization problem is known as a benchmark problem, and it has been studied by many researchers. The second problem is a 10-bay periodically assembled truss bridge. The optimization of the 10-bay truss bridge involves results with and without periodicity, and the total weights of both systems are compared.

Impulse response of the periodically assembled truss is studied experimentally and numerically. In the numerical study, different numbers of unit cell trusses are evaluated under impulse excitation for three different truss topologies in order to observe how periodic behavior changes with the truss assembly and topology. Certain numbers of unit cells are selected based on the

frequency domain analysis of the desired periodic behavior. Impulse response of the selected truss is analyzed for different levels of stiffness reduction in one diagonal member in each unit cell. In the experimental study, impulse responses of pristine and damaged condition of the truss are analyzed in time and frequency domains.

4.2 Findings

- The periodic behavior is affected by number of unit cells in a truss system. When number of unit cells are increased, the frequency spectrum of each adjacent cell in the same truss system has similar behavior, especially high frequency components. Lower frequency modes are more affected by boundary conditions. The impulse responses for different number of unit cells indicate that the periodic behavior is directly proportional to number of unit cells.
- The acceleration response of damaged unit cell increases with the increment of damage, while other undamaged unit cells behave similar to their pristine condition. The direct comparison of adjacent unit cells allows identifying the position of damaged unit cell.

4.3 Future Work

- Genetic algorithm optimization requires finite element analysis for structural optimization. However, standard finite element method is not convenient for an optimization of periodic structures. The optimization gives the best results regardless of a periodic configuration. For this reason, after the optimization, periodicity of the structure is degenerated. In order to avoid this, recursive finite element method can be used in genetic

algorithm. Recursive finite element method assembles only one periodic pattern in the finite periodic structure, and the entire structure is built by applying periodic boundary condition. This method will allow optimization for structures without losing periodicity. Since the recursive finite element method does require only one periodic pattern for modeling the entire system; number of elements in the model are reduced, thus the optimization process will take less time.

- The impulse responses experiments are performed using the impulse hammer, generating excitation source up to 8 kHz. However, higher frequency excitation results in better periodic behavior between unit cells. Currently, there is no commercially available impulse hammer with an excitation frequency higher than 20 kHz. An impulse hammer can be designed with an excitation frequency higher than 20 kHz using micro size hammer tip using micromachining technology.
- The impulse response method will be carried out in a field experiment using a truss bridge assembled with periodic unit cells.
- The Impulse response method studied in this research can be extended to 3D periodic systems such as space trusses. In order to record all the components of the acceleration response, triaxial accelerometers can be used.

CITED LITERATURE

1. Onwubolu, G. C. and Babu, B.: New optimization techniques in engineering, volume 141. Springer, 2013.
2. Farkas, J.: Structural optimization as a harmony of design, fabrication and economy. Structural and multidisciplinary optimization, 30(1):66–75, 2005.
3. Balling, R. J., Briggs, R. R., and Gillman, K.: Multiple optimum size/shape/topology designs for skeletal structures using a genetic algorithm. Journal of structural engineering, 132(7):1158–1165, 2006.
4. Yang, R. and Chuang, C.: Optimal topology design using linear programming. Computers & structures, 52(2):265–275, 1994.
5. Jameson, A.: Gradient based optimization methods. Technical report, MAE Technical Report, 1995.
6. Geem, Z. W., Kim, J. H., and Loganathan, G.: A new heuristic optimization algorithm: harmony search. Simulation, 76(2):60–68, 2001.
7. Izmailov, A. F. and Solodov, M. V.: Examples of dual behaviour of newton-type methods on optimization problems with degenerate constraints. Computational Optimization and Applications, 42(2):231–264, 2009.
8. Jenkins, W.: Towards structural optimization via the genetic algorithm. Computers & Structures, 40(5):1321–1327, 1991.
9. Holland, J. H.: Genetic algorithms. Scientific american, 267(1):66–72, 1992.
10. Goldberg, D.: Genetic algorithms in search, optimization and machine learning, 1989.
11. Farhat, F., Nakamura, S., and Takahashi, K.: Application of genetic algorithm to optimization of buckling restrained braces for seismic upgrading of existing structures. Computers & Structures, 87(1):110–119, 2009.

12. Walters, D. C. and Sheble, G. B.: Genetic algorithm solution of economic dispatch with valve point loading. IEEE transactions on Power Systems, 8(3):1325–1332, 1993.
13. Adeli, H. and Sarma, K. C.: Cost optimization of structures: fuzzy logic, genetic algorithms, and parallel computing. John Wiley & Sons, 2006.
14. Gätzi, R., Uebersax, M., and König, O.: Structural optimization tool using genetic algorithms and ansys. In Proc. 18. CAD-FEM Users Meeting, Internationale FEM-Technologietage, Graf-Zeppelin-Haus, Friedrichshafen, 2000.
15. Gen, M. and Cheng, R.: Genetic algorithms and engineering optimization, volume 7. John Wiley & Sons, 2000.
16. Schmit, L. A. and Farshi, B.: Some approximation concepts for structural synthesis. AIAA journal, 12(5):692–699, 1974.
17. Schmit, L. and Miura, H.: Approximation concepts for efficient structural synthesis. NASA contractor Report, 2552, 1976.
18. Venkayya, V.: Design of optimum structures. Computers & Structures, 1(1-2):265–309, 1971.
19. Sedaghati, R.: Benchmark case studies in structural design optimization using the force method. International Journal of Solids and Structures, 42(21):5848–5871, 2005.
20. Kaveh, A. and Rahami, H.: Analysis, design and optimization of structures using force method and genetic algorithm. International Journal for Numerical Methods in Engineering, 65(10):1570–1584, 2006.
21. Li, L., Huang, Z., Liu, F., and Wu, Q.: A heuristic particle swarm optimizer for optimization of pin connected structures. Computers & Structures, 85(7):340–349, 2007.
22. Farshi, B. and Alinia-Ziazi, A.: Sizing optimization of truss structures by method of centers and force formulation. international Journal of Solids and Structures, 47(18):2508–2524, 2010.
23. Aslani, M., Asla, R. N., Oftadehb, R., and Panahic, M. S.: A novel hybrid simplex-genetic algorithm for the optimum design of truss structures. In Proceedings of the world congress on engineering, volume 2, 2010.

24. Aashto, L.: Bridge design specifications 2014 aashto washington. DC, USA.
25. ANSI, A.: Aisc 360-16. Specification for Structural Steel Buildings. Chicago, IL, USA, 2016.
26. Matsumoto, Y., Yamaguchi, H., and Yoshioka, T.: A field investigation of vibration-based structural health monitoring in a steel truss bridge. In Proceedings of the IABSE-JSCE Joint Conference on Advances in Bridge Engineering-II, pages 8–10, 2010.
27. Ni, Y., Xia, H., Wong, K., and Ko, J.: In-service condition assessment of bridge deck using long-term monitoring data of strain response. Journal of Bridge Engineering, 17(6):876–885, 2011.
28. Elmasry, M., Shehadeh, M., and Attia, M.: Structural health monitoring of steel trusses using acoustic emission technique.
29. Romeo, F. and Ruzzene, M.: Wave propagation in linear and nonlinear periodic media: analysis and applications, volume 540. Springer Science & Business Media, 2013.
30. Brun, M., Movchan, A. B., and Jones, I. S.: Phononic band gap systems in structural mechanics: finite slender elastic structures and infinite periodic waveguides. Journal of Vibration and Acoustics, 135(4):041013, 2013.
31. Grima, J. N., Attard, D., and Gatt, R.: Truss-type systems exhibiting negative compressibility. physica status solidi (b), 245(11):2405–2414, 2008.
32. Hutchinson, R. and Fleck, N.: The structural performance of the periodic truss. Journal of the Mechanics and Physics of Solids, 54(4):756–782, 2006.
33. Logan, D. L.: A first course in the finite element method. Cengage Learning, 2011.
34. Chopra, A. K. et al.: Dynamics of structures, volume 4. Prentice Hall New Jersey, 2007.

VITA

Mr. Onur Can graduated from Istanbul Technical University with a Bachelors of Science in Civil Engineering. Mr. Can is currently a graduate student at University of Illinois at Chicago. Mr. Can worked on National Science Foundation project: “CAREER: Engineered Spatially Periodic Structure Design Integrated with Damage Detection Philosophy”. The project includes early damage detection of periodically assembled truss systems using impulse response method. Mr. Can will earn Master of Science degree from University of Illinois at Chicago in 2017.